Expression levels of E-cadherin in breast cancer cells alter apoptotic susceptibility and facilitate cancer stem cell phenotypes in response to Wnt signalling

Sarah Ooi

Thesis submitted to the

Faculty of Graduate and Postdoctoral Studies

in partial fulfillment of the requirement for the degree of

Master of Science in Biochemistry

Department of Biochemistry, Microbiology and Immunology

Faculty of Medicine

University of Ottawa

ABSTRACT

It is well established that the Wnt pathway is associated with tumorigenesis in a wide range of human cancers, including a majority of breast cancers. However, due to diverse roles of Wnt signalling, therapeutic targeting has not yielded consistent results and underlying mechanisms remain unclear. Here, I show that breast cancer cell lines with high E-cadherin expression are resistant to TCF4 inhibitors and develop cancer stem cell characteristics. Conversely, cells with low levels of E-cadherin are very susceptible to cell death with the same treatment. My results suggest that breast cancer cells in an epithelial-like state, but not mesenchymal-like state, will be more responsive to therapeutic targeting of the Wnt/TCF pathway. Importantly, E-cadherin high cells show robust Akt activation, whereas E-cadherin low cells do not. Thus, combinational inhibition of both Wnt and Akt signalling is needed to effectively target breast cancer cells in both the epithelial and mesenchymal states.

ACKNOWLEDGEMENTS

I would like to thank my supervisor, Dr. Lisheng Wang, for his invaluable source of guidance and knowledge. To current and previous lab members, especially Dr. Deyong Jia, Yuan Tan, and Dr. Li Li, I greatly appreciate all of the support and encouragement given throughout my time here; it was a pleasure to work amongst friends. Also deserving special thanks is my thesis advisory committee, Dr. Jonathan Lee and Dr. Christina Addison, whose assistance and input have helped a great deal during the course of my research. I would like to give a notable mention to The Breast Cancer Research Foundation for funding opportunities and making this research possible.

TABLE OF CONTENTS

LIST OF ABBREVIATIONS

CSCs: Cancer Stem Cells

ALDH: ALdehyde DeHydrogenase

EMT: Epithelial to Mesenchymal Transition

iPSC: induced Pluripotent Stem Cell

MET: Mesenchymal to Epithelial Transition

PI3K: PhosphoInositide 3-Kinase

APC: Adenomatous Polyposis Coli

GSK-3: Glycogen Synthase Kinase 3

TCF: T Cell Factor

LEF: Lymphoid Enhancer-binding Factor

LRP5/6: Low-density lipoprotein Receptor-related Proteins 5/6

CBP: CREB-Binding Protein

TBP: TATA-Binding Protein

RTK: Receptor Tyrosine Kinase

PIP3: PhosphatidylInositol (3,4,5)-trisPhosphate

IRS: Insulin Receptor Substrate

DMEM: Dulbecco's Modified Eagle's Medium

siRNA: Small Interfering RNA

DMSO: Dimethyl Sulfoxide

MTT: thiazolyl blue tetrazolium bromide

PBS: Phosphate Buffered Saline

RT-qPCR: Quantitative Reverse Transcription PCR

GAPDH: GlycerAldehyde 3-Phosphate DeHydrogenase

BSA: Bovine Serum Albumin

TBST: Tris-Buffered Saline Tween-20

PARP (-T/C): Poly ADP-Ribose Polymerase (-total/cleaved)

ECL: Enhanced Chemiluminescence System

FACS: Fluorescence-Activated Cell Sorting

7-AAD: 7-Amino-actinomycin D

SE: Standard Error

LIST OF FIGURES

LIST OF TABLES

1. INTRODUCTION

1.1 Breast cancer and cancer stem cells

Although there have been many advances in cancer research, breast cancer is still the second leading cause of death in women (1). Most of the problem lies within cancer therapy itself. Currently, treatment consists of tumour removal through surgery followed by adjuvant therapy consisting of radiation, chemotherapy, hormonal therapy, and/or biological therapy. However, although these methods are successful in removing the bulk of the tumour, chance of relapse is still high with 36.8% of survivors suffering recurrence within 10 years (2). Recurrence generally occurs when a small population of cancer cells resists treatment and persists, and there is now an increasing amount of evidence to suggest that these are cancer stem cells (CSCs) (3, 4).

The cancer stem cell hypothesis states that a tumour is maintained through CSCs that can both self-renew and differentiate to constitute the bulk of the tumour (5–7). Several studies have now shown that cell populations enriched for CSCs can form tumours in immunocompromised mice that reproduce the molecular heterogeneity of the original malignancy (8–11). Not only do CSCs have self-renewal and differentiation capabilities, similar to normal tissue stem cells, but are also more resistant to conventional cancer therapies as shown *in vitro* and *in vivo* studies (12–15). There are a number of ways in which CSCs can achieve this resistance, including stem cell quiescence, increased drug efflux pumps, protected niche environments, and enhanced repair/survival pathways (16–21). Despite initial progress being made into the identification and characterization of CSCs,

specifically targeting these cells continues to be an issue. The first challenge involves identifying markers specific to CSCs. Al-Hajj *et al.* was the first group to isolate breast CSCs using the marker $CD44^{+}/CD24^{-/low}/Lineage^{-}$, which categorized a small population of cells that were able to form new tumours in non-obese diabetic/severe combined immunodeficiency mice (9). Later, aldehyde dehydrogenase (ALDH) was also identified as a potent marker for CSCs in breast cancer (22). Both $CD44^{+}/CD24^{-}$ and $ALDH^{+}$ are now common markers used to characterize CSCs in breast and other forms of cancer. Unfortunately, however, neither marker can be used exclusively or conclusively to identify the entire population of breast CSCs (23, 24). The second challenge involves developing therapeutics that specifically and effectively target these CSCs that are otherwise resistant to conventional therapies. As mentioned earlier, there are a number of theories regarding the method of CSC resistance to treatment, and as a result, all of these avenues are being explored without clear knowledge of which will prove to be most effective. While the concept of CSCs is not new, it has only recently been at the forefront of cancer research and we can only continue to gain novel insights into the inner workings of CSCs, all of which will help with future therapeutics.

1.2 Epithelial to mesenchymal or mesenchymal to epithelial; which way to go?

Cancer cells commonly undergo an epithelial to mesenchymal transition (EMT) in order to disseminate and metastasize (4, 25). Whereas an epithelial phenotype is associated with apical-basal polarity, tight junctions, and cell-cell adhesion markers, mesenchymal cancer cells lack polarity and have migratory and invasive properties, allowing metastasis from a primary heterogeneous tumour through the extracellular membrane to a secondary site (4, 25, 26). Since recurrence is often associated with metastasis, it led to the theory that CSCs were metastatic mesenchymal cells (9, 27–30). Several papers are now reporting that CSCs display plasticity and interconvert between EMT and MET (mesenchymal to epithelial transition), based on environmental and intracellular clues, and that MET is crucial for metastatic outgrowth (31–36). This process is illustrated in Figure 1, which shows a small population of cells in the primary tumour undergoing EMT and either recurring locally or intravasating into the blood or lymphatic vessel. After extravasation at a distant site, cells undergo MET for colonization and growth of a secondary tumour.

One major player in the conversion from epithelial to mesenchymal and vice versa, is E-cadherin (34, 35, 37). E-cadherin is heavily involved in the epithelial phenotype and loss of E-cadherin is indicative of a mesenchymal phenotype (Figure 1). In fact, constitutive production or loss of E-cadherin *in vivo* has been shown to induce MET or EMT in cancer cells, respectively (31, 33, 38–41). Fluctuating E-cadherin levels in tumours are typically controlled through epigenetic mechanisms, such as transcriptional repression and promoter hypermethylation (42–45). As interconversion between EMT and MET in CSCs is a new theory, most research thus far has focused on E-cadherin as being a tumour suppressor and

possible means to restore E-cadherin mediated cell adhesion. For example, Witta *et al*. found that restoring E-cadherin in lung cancer led to increased sensitivity to epidermal growth factor receptor inhibitors and apoptosis in previously resistant cell lines (46). Tryndyak *et al*. used miR-200-induced up-regulation of E-cadherin to decrease invasiveness and increase sensitivity to chemotherapeutic agent doxorubicin in breast cancer cells (47). Similarly, Nam *et al*. restored the E-cadherin-mediated cell adhesion system by treatment with Src family kinase inhibitor PP2, leading to the reduction of cancer metastasis (48). Conversely, alternative roles for E-cadherin in tumour progression are emerging, such as tumorsphere formation and collective cancer metastasis (49, 50). In ovarian cancer and invasive ductal carcinoma, E-cadherin is highly expressed in the majority of tumours and maintains expression during metastasis (51–53). Additionally, our group found that E-cadherin actively contributed to the self- renewal and pluripotency gene expression of human embryonic stem cells (54, 55). Furthermore, E-cadherin has been shown to activate phosphoinositide 3-kinase (PI3K) through recruitment to E-cadherin-containing protein complexes, and activating downstream signalling proteins such as Akt (56–58). It is clear that a full understanding of CSCs, including the role of EMT/MET, E-cadherin, and the signalling pathways involved, will be needed to specifically target this elusive cancer cell population.

Figure 1. EMT-MET conversion and the contribution of E-cadherin. When a primary tumour undergoes invasion (1), cells convert from an epithelial to mesenchymal phenotype (EMT), which is characterized by a loss of E-cadherin (2). Cells can then relocalize (4) or intravasate (5) into the blood stream, leading to extravasation (7), mesenchymal to epithelial reversion (MET), and metastasis (9) at a secondary site in the body. [Modified from Thompson and Haviv. 2011 Nat Med 17:1048 (59)]

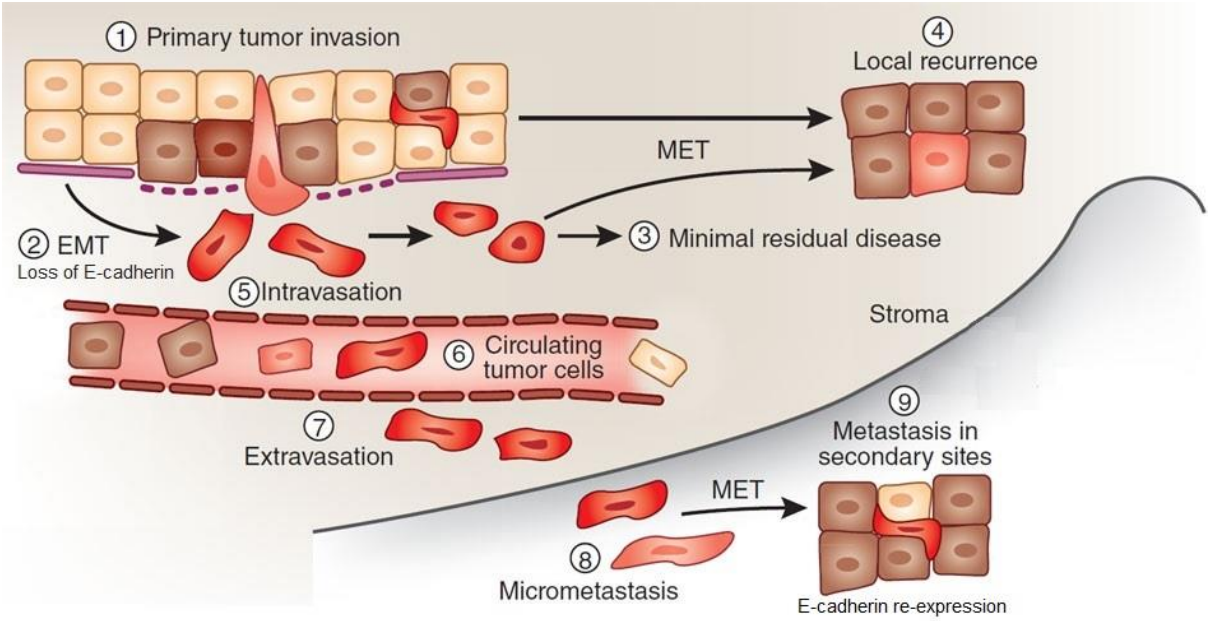
① Primary tumor invasion
④ Local recurrence
MET
② EMT
Loss of E-cadherin
③ Minimal residual disease
⑤ Intravasation
Stroma
⑥ Circulating tumor cells
⑦ Extravasation
⑨ Metastasis in secondary sites
MET
⑧ Micrometastasis
E-cadherin re-expression

1.3 Wnt signalling pathway

The Wnt family of glycoproteins are able to activate either the canonical (dependent on nuclear β-catenin) or non-canonical pathway. Activation of the canonical pathway (Figure 2) leads to inhibition of the β-catenin destruction complex, consisting of axin, adenomatous polyposis coli (APC), protein phosphatase 2A, CK1-α and glycogen synthase kinase 3 (GSK-3), and subsequent translocation and accumulation of β-catenin in the nucleus. In the nucleus, β-catenin forms a complex with transcription factors that includes the T cell factor (TCF)/lymphoid enhancer-binding factor (LEF) family. Altogether, this complex is able to activate transcription for numerous genes, including core factors known to be associated with pluripotency induction (Sox2, c-Myc, Nanog, Oct4, Klf4) (60–63). Not only is β-catenin a pivotal factor of the Wnt signalling pathway, but it is also an intracellular adaptor of E-cadherin (64, 65). This leads to competition for cytoplasmic β-catenin, where increased E-cadherin levels sequester β-catenin to the membrane, and as a retaliation, Wnt transcription products include proteins that inhibit E-cadherin expression (e.g. Snail/Slug) (66–69).

It is well established that the Wnt pathway is associated with tumorigenesis in a wide range of human cancers (70). However, due to diverse roles of Wnt signalling in cellular regulation, activation can either fuel or repress tumour growth depending on yet to be determined aspects of the molecular pathways that are expressed (71). Specifically, there is great deal of controversy over whether Wnt maintains pluri-/multipotency or induces differentiation (72–75). It likely involves input from various sources, such as growth factors, cytokines and hormones, ionic concentrations, genetic mutations, adhesion, etc., and cell fate will ultimately depend on cell type, cancer stage, and tumour grade (76). In breast cancer,

there is strong evidence for overexpression of various Wnt proteins that signal through the canonical pathway, as well as nuclear/cytoplasmic accumulation of β-catenin, both of which have not been observed in normal tissue (77–79). Furthermore, Wnt has been implicated in many facets of breast tumour development and growth, and inhibition has been shown to prevent migration and proliferation, enhance chemosensitivity and induce apoptosis (80–83). For this reason, Wnt signalling looks to be a promising target to control both tumour growth and metastasis, and further insights into the regulation, interactions, and outcomes, will help to advance future therapeutic treatments.

Figure 2. Wnt signalling pathway. Depiction of the canonical (β-catenin dependant) Wnt signalling pathway. LRP5/6-Frizzled receptors bind to Wnt protein leading to inhibition of the β-catenin destruction complex, consisting of GSK-3β, APC, and Axin. β-catenin is then able to accumulate in the cytoplasm and can interact with cadherin junctions at the membrane and/or transfer into the nucleus to interact with transcription factors, such as LEF/TCFs, CREB-binding protein (CBP)/p300, and TATA-binding protein (TBP). Activation of the Wnt pathway leads to transcription of downstream Wnt signalling proteins (c-Myc, Cyclin D, c-jun, etc.) involved in regulation and cell fate. [Modified from Howard *et al.* 2003 Bmc Musculoskelet Disord 4:16 (84)]

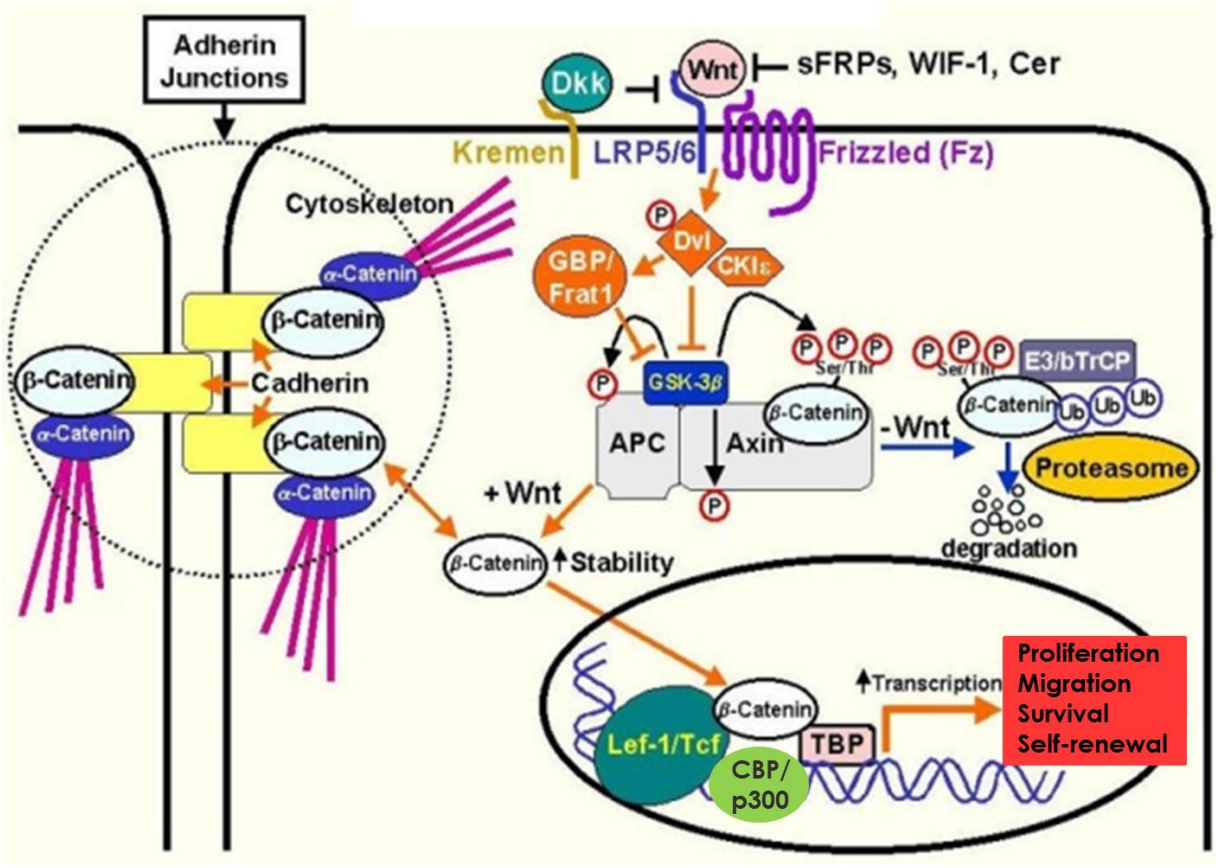
Adherin Junctions
Dkk
Wnt
sFRPs, WIF-1, Cer
Kremen
LRP5/6
Frizzled (Fz)
Cytoskeleton
α-Catenin
β-Catenin
Cadherin
β-Catenin
α-Catenin
β-Catenin
α-Catenin
P
Dvl
CKIε
GBP/ Frat1
GSK-3β
APC
Axin
β-Catenin
Ser/Thr
E3/bTrCP
Ub
-Wnt
Proteasome
degradation
+ Wnt
β-Catenin
Stability
Transcription
β-Catenin
Lef-1/Tcf
TBP
CBP/ p300
Proliferation
Migration
Survival
Self-renewal

1.4 Akt signalling pathway

Akt remains in the cytosol in an inactive conformation until it is recruited to the membrane and activated by serine/threonine kinases, mainly PI3K (Figure 3). Upon growth factor or hormone binding, receptor tyrosine kinases (RTKs), dimerize and cross-phosphorylate intracellular domain tyrosine residues. Regulatory subunit p85 binds to these residues or adaptor proteins and recruits the catalytic subunit p110, forming active PI3K, which in turn catalyzes the formation of phosphatidylinositol (3,4,5)-trisphosphate (PIP_3). Akt has a high affinity for PIP_3 and translocates to the membrane. Interaction causes a conformational change in Akt that exposes Thr308 and Ser473 for consequent phosphorylation and activation. Interaction and phosphorylation of downstream signalling pathways enable regulation of survival, growth, proliferation, cell migration, glucose metabolism and angiogenesis; all of which are hallmarks of cancer (85–88).

Consequently, Akt activation in many cancers makes it a target for intense therapeutic efforts. Hyperactive Akt activation is commonly achieved through mutations to the genes encoding Akt and upstream activators, deletion or inactivation of tumour suppressors such as phosphatase and tensin homolog, tuberous sclerosis complex 2, and liver kinase B1, or overexpression of downstream effectors such as eukaryotic initiation factor 4E (89–96). Evidently, several drugs have been developed to target Akt's various points of regulation, some of which are currently in clinical trials. For example, there are PIP3 analogues to block binding to Akt's PH domains, alkylphospholipids to prevent membrane localization, selective inhibitors to target Akt activation, etc. (97–103) Further study will determine which inhibitor types/combinations are most effective for future cancer treatments.

Figure 3. Akt signalling pathway. Depiction of the Akt signalling pathway. Stimulation of RTK results in cross-phosphorylation of its intracellular domains. Binding of the p85 subunit either directly or indirectly (ex. insulin receptor substrate (IRS)) leads to the recruitment of the p110 subunit, forming activated PI3K. PI3K catalyzes the formation of PIP_3, leading to the recruitment of Akt to the membrane and its conformational change. Fully activated Akt is achieved through phosphorylation. Akt interacts with and phosphorylates numerous downstream proteins to regulate survival, growth, proliferation, cell migration, glucose metabolism and angiogenesis. [Modified from Vivanco and Sawyers. 2002 Nat Rev Cancer *2*:489 (88)]

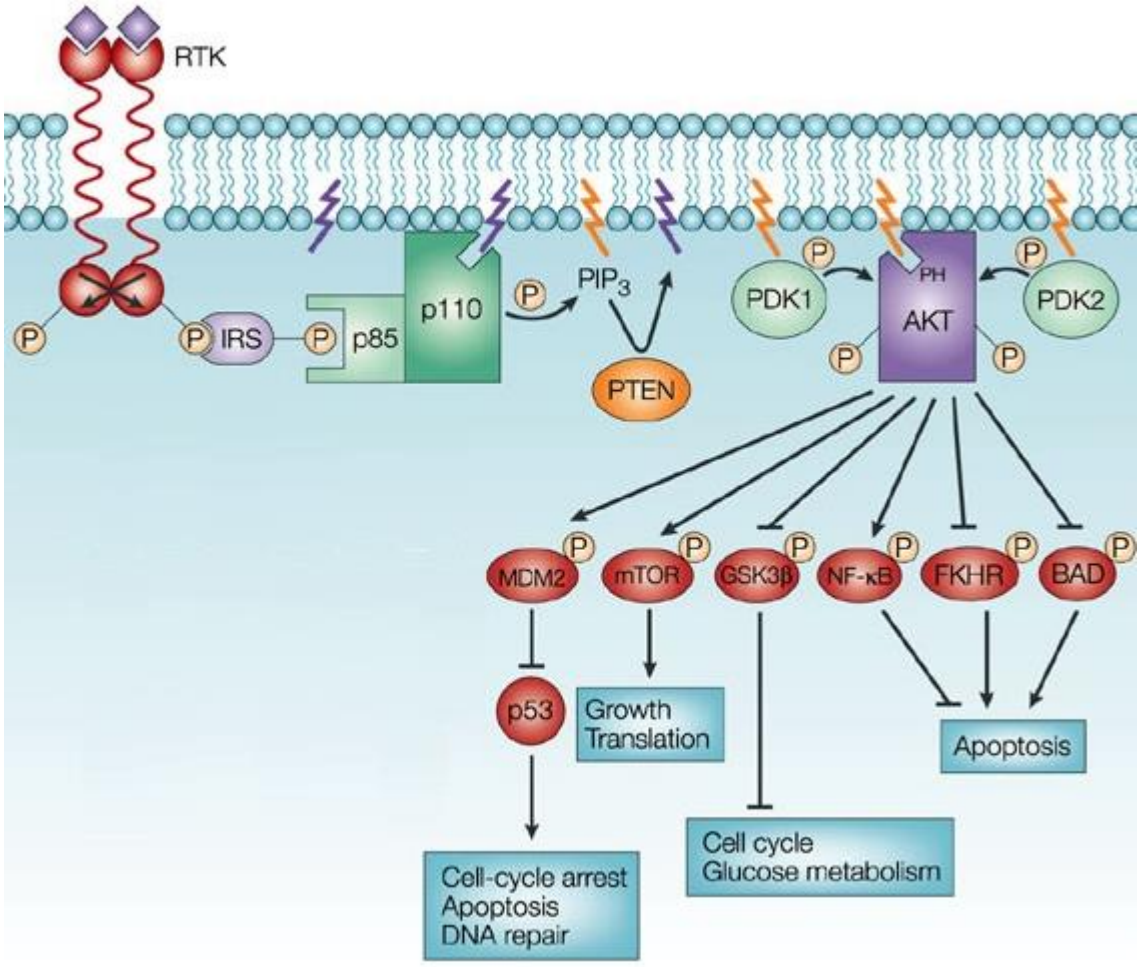
RTK
P
IRS
P
p85
p110
P
PIP3
PTEN
PDK1
P
PH
AKT
P
P
PDK2
P
MDM2
P
mTOR
P
GSK3β
P
NF-κB
P
FKHR
P
BAD
P
p53
Growth
Translation
Apoptosis
Cell cycle
Glucose metabolism
Cell-cycle arrest
Apoptosis
DNA repair

1.5 Hypothesis and the aim of this study

Although E-cadherin competes with Wnt for β-catenin levels and it is established that Wnt products encode proteins that down-regulate E-cadherin, little is known about what effects E-cadherin has on Wnt signalling. Evidence has already shown that E-cadherin's role in the cell is more profound than solely adhesion, however mechanisms behind how an adhesion molecule with unknown enzymatic activity is able to elicit downstream signals still remains unclear. If E-cadherin is to be a candidate for cancer therapeutics, a better understanding of its influence on different signalling pathways will help determine if upregulating/downregulating E-cadherin would lead to tumour growth or regression.

I hypothesized that the expression level of E-cadherin, and therefore a mesenchymal/epithelial state, influences whether Wnt inhibitors facilitate cell death or cancer stem cell formation in breast cancer. In support of this hypothesis, I sought to examine the effects that Wnt inhibitors had on cell lines with little to no expression or overexpression of E-cadherin (Objective 1); define whether Wnt inhibitor BC21 caused apoptosis in E-cadherin low cell lines (Obective 2); determine if BC21 induced a cancer stem cell phenotype in E-cadherin high cell lines (Objective 3); identify the means by which E-cadherin confers resistance and CSC characteristics in E-cadherin high cells (Objective 4) and verify that targeted therapy based on E-cadherin expression levels can effectively eliminate cancer cell populations (Objective 5). This research will help define the role of E-cadherin in breast cancer progression and provide new insights into treatment avenues. Ultimately, I hope to eradicate tumours through targeted therapy based on E-cadherin expression.

2. MATERIALS & METHODS

2.1 Cell and culture conditions

MDA-MB-231 and MCF7 human breast cancer cell lines were obtained from ATCC (#HTB-26 and #HTB-22, respectively). These are adherent epithelial cell lines derived from metastatic adenocarcinoma. However, MDA-MB-231 is a triple negative aggressive cell line with a spindle morphology, whereas MCF7 is an estrogen and progesterone receptor positive line with a spherical morphology. Both cell lines were cultured at 37°C and 5% CO_2 atmosphere in flasks/plates (Corning) maintained in Dulbecco's Modified Eagle's Medium (DMEM) high glucose media (Thermo Fisher) supplemented with 10% fetal bovine serum and 1% penicillin/streptomycin (Thermo Fisher). MDA-MB-231 cells were passaged every 3 days at a 1:10 split ratio, and MCF7 cells were passaged every 7 days at a 1:4 split ratio by dissociation with 1 mL 0.05% trypsin-EDTA (Thermo Fisher) for 3 minutes. The day on which cells were seeded was defined as day 0.

2.2 Tet-On® Advanced Inducible Gene Expression System

MDA-MB-231 cells were transfected with pLVX-Tet-On Advanced and pLVX-Tight-Puro according to manufacturer's instructions (Clontech). MDA-MB-231 E-cadherin^{low} cells were generated using an empty vector of pLVX-Tight-Puro, while MDA-MB-231 E-cadherin^{high} cells were generated using pLVX-Tight-Puro containing an E-cadherin gene insert. Stable clones were selected after 3 days using G418 (Clontech) at a concentration of 1000 µg/mL for selection and 400 µg/mL for maintenance and Puromycin dihydrochloride (Thermo Fisher) at a concentration of 1 µg/mL for selection and 0.5 µg/mL for maintenance. E-

cadherin expression was activated by adding 1 µg/mL doxycycline hydrochloride (Thermo Fisher) to the cell culture every 2-3 days. E-cadherin levels were examined following RNA extraction by qPCR analysis and protein knock-down levels were examined by western blotting.

2.3 Small interfering RNA (siRNA) transfection

MCF7 cells in 12-well plates were transiently transfected with 20 nM Silencer Select pre-designed E-cadherin siRNA (#4392420 Thermo Fisher) or with 20 nM Silencer Select Negative Control #1 siRNA (#4390843 Thermo Fisher) using Lipofectamine RNAi MAX (Thermo Fisher) as per manufacturer's recommendation.

1 µL of siRNA were diluted in 100 µL of Opti-MEM (Thermo Fisher) and incubated at room temperature for 5 minutes, then combined with 1 µL lipofectamine, which was also diluted in 100 µL Opti-MEM. The siRNA:lipofectamine mixture was incubated for 20 minutes at room temperature, then added drop wise to wells containing 800 µL Opti-MEM and mixed gently by rocking back and forth. 12 to 24 hours post-transfection, the media was replaced with fresh Opti-MEM and the transfection process repeated for a second time. siRNA mediated knock-down of E-cadherin transcript levels were examined following RNA extraction by qPCR analysis and protein knock-down levels were examined by western blotting, 24 and 72 hours post double-transfection, respectively. Transfection efficiency was estimated by measuring the change in expression levels with or without E-cadherin siRNA, by looking at fold change for qPCR and densitometry (ImageJ) for Western blot.

2.4 Inhibitor treatments

BIO – GSK-3 inhibition was achieved using BIO inhibitor (#361550 EMD Millipore) that blocks GSK-3 mediated degradation of β-catenin. Stock solutions of BIO inhibitor were reconstituted in DMSO (dimethyl sulphoxide) as per manufacturer's recommendation and stored at 10 mM concentration at 4°C protected from light. Toxicity was verified by treating cells at various concentrations (1-7.5 µM) for 1-4 days and determined by counting live and dead cells using a haemocytometer following trypan blue (Thermo Fisher) staining. Cells were treated with 2.5 µM BIO every day with medium change for 4 days, with an equivalent volume of DMSO used as a vehicle control.

NOTE: CHIR-99021 was used as a replacement for BIO as a GSK-3 inhibitor for flow cytometry experiments, as BIO stained cells red and skewed results. Stock solutions of CHIR-99021 inhibitor (#SML1046 Sigma-Aldrich) were reconstituted in DMSO as per manufacturer's recommendation and stored at 10 mM concentration at -20°C protected from light. Toxicity was verified by treating cells at various concentrations (1-7.5 µM) for 4 days and determined by counting live and dead cells using a haemocytometer following trypan blue staining. Cells were treated with 5 µM CHIR-99021 every day with medium change for 4 days, with an equivalent volume of DMSO used as a vehicle control.

IQ-1 – p300 inhibition was achieved using IQ-1 inhibitor (#412400 EMD Millipore) that blocks the interaction between β-catenin and transcription factor p300. Stock solutions of IQ-1 inhibitor were reconstituted in DMSO as per manufacturer's recommendation and stored at

10 mM concentration at -20°C protected from light. Toxicity was verified by treating cells at various concentrations (2-6 µM) for 1-4 days and determined by counting live and dead cells using a haemocytometer following trypan blue staining. Cells were treated with 5 µM IQ-1 every day with medium change for 4 days, with an equivalent volume of DMSO used as a vehicle control.

ICG-001 – CBP inhibition was achieved using ICG-001 inhibitor (#847591 EMD Millipore) that blocks the interaction between β-catenin and transcription factor CBP. Stock solutions of ICG-001 inhibitor were reconstituted in DMSO as per manufacturer's recommendation and stored at 25 mM concentration at -20°C protected from light. Toxicity was verified by treating cells at various concentrations (5-25 µM) for 1-4 days and determined by counting live and dead cells using a haemocytometer following trypan blue staining. Cells were treated with 5 µM ICG-001 every day with medium change for 4 days, with an equivalent volume of DMSO used as a vehicle control.

BC21 – TCF4 transcription factor inhibition was achieved using BC21 inhibitor (#219334 EMD Millipore) that blocks the interaction between TCF4 and β-catenin. Stock solutions of BC21 inhibitor were reconstituted in DMSO as per manufacturer's recommendation and stored at 5 mM concentration at -20°C protected from light. Toxicity was verified by treating cells at various concentrations (1-10 µM) for 1-4 days and determined by counting live and dead cells using a haemocytometer following trypan blue staining. Cells were treated with 5

µM BC21 every day with medium change for 4 days, with an equivalent volume of DMSO used as a vehicle control.

Akt VIII – Akt inhibition was achieved using Akt VIII inhibitor (#124018 EMD Millipore) that allosterically blocks Akt. Stock solutions of Akt VIII inhibitor were reconstituted in DMSO as per manufacturer's recommendation and stored at 9 mM concentration at -80°C protected from light. Toxicity was verified by treating cells at various concentrations (0.5-10 µM) for 1-4 days and determined by counting live and dead cells using a haemocytometer following trypan blue staining. Cells were treated with 3 µM Akt VIII every day with medium change for 4 days, with an equivalent volume of DMSO used as a vehicle control.

2.5 Cell counting assays

Cells were washed twice with phosphate-buffered saline (PBS) and dissociated with 0.05% trypsin-EDTA. Live cells were counted using trypan blue staining in a hemocytometer.

Cell viability levels were determined by conducting a MTT (thiazolyl blue tetrazolium bromide) assay. MTT (Sigma-Aldrich) diluted at 5 mg/mL in PBS was added to cells in a 96 well flat bottom plate (Corning) in a 1:10 ratio and incubated at 37°C for 4 hours. Cells were spun down at 4000 rpm for 5 minutes (CR3i, Thermo Fisher), media removed, and resuspended in 150 µL DMSO for 30 minutes to terminate the reaction and lyse cells. Optical density was measured at 490 nm using the Synergy H1 (Biotek).

2.6 Quantitative reverse transcription PCR (RT-qPCR)

Total RNA was extracted from MDA-MB-231 and MCF7 cells using RNeasy Mini Kit (Qiagen) and quantitated using NanoDrop 1000 (Thermo Fisher) and the RNA quality was ensured by spectrophotometric analysis ($A_{260/280}$)(NanoDrop). cDNA was generated using 500 ng of total RNA with the iScript cDNA Synthesis Kit (Bio-Rad) and GeneAmp PCR System 2700 (R&D Systems). qPCR was performed using SYBR Green Supermix (Bio-Rad) on MyiQ System (Bio-Rad). Approximately 10 ng of cDNA was used per individual reaction with primer concentrations of 5 µM. Amplifications were performed using the following conditions: 94°C, 1m30s and 40 cycles 94°C, 10s; 60°C, 30s; 72°C, 30s. All data was normalized to glyceraldehyde 3-phosphate dehydrogenase (GAPDH) using the ΔΔCT method (104). pPCR was performed using human-specific primers listed in Table 1. All primers were designed by Deyong Jia or Anna Jesierski using PrimerQuest from Integrated DNA Technologies.

Table 1. List of primer sequences.

Primer	Sequence	Product Size
GAPDH	Forward: 5'-ACAGTCAGCCGCATCTTCTT-3' Reverse: 5'-GACAAGCTTCCCGTTCTCAG-3'	259
E-cadherin	Forward: 5'-TGCCCAGAAAATGAAAAAGG-3' Reverse: 5'-GGATGACACAGCGTGAGAGA-3'	225
p21	Forward: 5'-GGACAGCAGAGGAAGACCATGTG-3' Reverse: 5'-GATCAGCCGGCGTTTGGAGTGGTA-3'	164
Caspase-3	Forward: 5'-TGATGATGTGGAAGAACTTAGG-3' Reverse: 5'-ACGGCTCCGCACCTGCTGAGGC-3'	943

2.7 Western blot assays

Cells were washed with ice-cold PBS and lysed directly on the tissue culture plate with TNEN lysis buffer containing 1X protease inhibitors (Sigma-Aldrich). Samples were normalized with protein assay dye (Bio-Rad) using a spectrophotometer measuring at 595λ (Beckman DU-600), then diluted 4:1 with 5X loading buffer for a total loading volume of 30 µL. Samples were run on a 10% sodium dodecyl sulfate polyacrylamide gel electrophoresis (80 volts for 1 hour then 120 volts for 1 hour) alongside a PageRuler Plus protein ladder (#26619 Thermo Fisher), and transferred to a polyvinylidene difluoride membrane (Bio-Rad) using a wet transfer apparatus (Bio-Rad) at 300 mA for 2 hours at 4°C. Membranes were blocked with 5% skim milk (Santa Cruz) or 5% bovine serum albumin (BSA) (Thermo Fisher) in TBST (tris-buffered saline containing 0.1% Tween-20, Sigma-Aldrich)) for 1 hour at room temperature and incubated with primary antibodies overnight at 4°C with gentle rocking. Cell lysates were assessed using E-cadherin mouse mAb (#1416 Abcam, 1:1000), poly ADP ribose polymerase-total (PARP-T)/PARP-cleaved (PARP-C)(Asp214)-rabbit mAb (#9532/5625 Cell Signaling, 1:1000), c-Myc rabbit mAb (#5605 Cell Signaling, 1:1000), Oct3/4 rabbit pAb (#137427 Abcam, 1:1000), Klf4 rabbit pAb (#72543 Abcam, 1:1000), Akt-phospho (Ser473)/Akt-total rabbit mAb (#4060/9272 Cell Signaling, 1:1000), and α-tubulin mouse mAb (#T9025 Sigma-Aldrich, 1:5000) as a loading control were diluted in TBST containing 5% skim milk or 5% BSA. Membranes were washed 3X for 15 minutes per wash in TBST. Secondary antibodies, goat anti-rabbit (#170-6515 Bio-Rad) and goat anti-mouse IgG-HRP-conjugates (#HAF007 R&D Systems), were diluted in 5% skim milk or 5% BSA (1:10000) and the membranes were incubated for 1 hour at room temperature with gentle rocking. Membranes were washed 3X for 15 minutes per wash in TBST. Membranes

were detected using the enhanced chemiluminescence system (ECL) (Select™, GE Healthcare). The ECL signal was detected using autoradiography film (Denville Scientific) and cassette.

2.8 Flow cytometry

Cells were dissociated into a single cell suspension, washed with PBS (GE Healthcare), counted with trypan blue and $1x10^6$ cells were resuspended in 100 µL fluorescence-activated cell sorting (FACS) buffer in 96-well U-bottom plates. Cells were incubated with 1.5 µL IgG (block Fc receptor) for 5 minutes at 4°C then stained with 1.5 µL CD44/CD24 (BD Biosciences) surface markers, as well as apoptosis marker Annexin V (eBioscience) for 30 minutes at 4°C in the dark. Plates were centrifuged at 4000 rpm for 4.5 minutes at 4°C and washed 3x with 200 µL FACS buffer. The samples were kept at 4°C in 200 µL FACS buffer and protected from light for 0 to 3 hours. Before analysis, 1.5 µL of viability stain 7-amino-actinomycin D (7-AAD) (eBioscience) was added then incubated for 10 minutes in the dark. Samples were then transferred to FACS tubes and 0.5 mL of isotone sheath fluid was added before flow cytometry with Beckman Cyan flow cytometer measuring 15000 events using FL2, 8, 5, and 4 channels, respectively, and analysis with Kaluza software (Beckman Coulter).

2.9 Colony formation assays

Cells were trypsinized, strained (Corning), and normalized to 5000 cells per well in a 12 well plate. The base layer consisted of 0.6% agarose (Sigma-Aldrich) plus 1X DMEM with supplements and cooled at room temperature for 5 minutes to allow agarose to solidify. Cells were added to the top layer, which consisted of 0.35% agarose plus 1X DMEM with supplements. Plates were incubated at 37°C for 21 days and fed with 300 µL DMEM media every 2-3 days. Cells were counted under a light microscope by adding 200 µL MTT/well and only including spheres that measured ≥ 100 µm in size.

2.10 Statistical analysis

Results are expressed as mean ± Standard Error (SE). Statistical significance was determined using a Student's *t*-test or ANOVA wherever appropriate. Results were considered significant when $p < 0.05$ (one asterisk) or < 0.01 (two asterisks). All experiments have at least three biological repeats (n=3).

3. RESULTS

3.1 Overexpression or knock-down of E-cadherin results in opposing outcomes when treated with Wnt inhibitors.

Protein fluctuation levels are common among cells depending on activity level, function, stress, etc., and E-cadherin is no exception. To emulate the fluctuating levels of E-cadherin in cancer cells undergoing EMT-MET, I used two commercially available cell lines, MDA-MB-231 and MCF7, which are derived from human breast cancer patients. MDA-MB-231 is a triple negative mesenchymal-like cell line with very low baseline levels of E-cadherin. In contrast, MCF7 is an estrogen/progesterone receptor positive epithelial cell line with high baseline levels of E-cadherin. To achieve differing E-cadherin levels within the same cell line, MDA-MB-231 cells were transfected with a Tet-On plasmid that activates E-cadherin expression when exposed to doxycycline (Figure 4) and MCF7 cells were knocked down with E-cadherin specific siRNA. Thus providing E-cadherin high systems, herein referred to as MDA-Ecad^{high} and MCF7-scrambled, and E-cadherin low systems, herein referred to as MDA-Ecad^{low} and MCF7-si-Ecad. E-cadherin expression was assessed at the transcript level (Figure 5A) and protein level (Figure 5B) for both cell lines.

Currently, there is no clear role for Wnt signalling in promoting or preventing cancer growth, and signalling outcomes have been found to be largely cancer stage-specific and type-specific. Therefore, MDA-MB-231 cells were tested against various Wnt pathway inhibitors to determine if a mesenchymal or epithelial phenotype, as represented by MDA-Ecad^{low} and MDA-Ecad^{high}, respectively, would alter the cell's response to Wnt signalling (Figure 6).

β-catenin/p300 inhibitor IQ-1 caused very little to no cell death in either cell line (cell counting data not shown). β-catenin/CBP inhibitor ICG-001 caused moderate cell death in MDA-Ecad^{low} cells (cell counting data not shown). Lastly, TCF4 inhibitor BC21 showed marked differences in the survival between E-cadherin low and E-cadherin high cells. Therefore, focus was placed on TCF4 inhibition and the mechanism behind differing survival patterns.

Figure 4. Generation of E-cadherin expression in MDA-MB-231 cell line. Schematic of the lentivirus used to generate MDA-MB-231 Tet-On E-cadherin^{low} (MDA-Ecad^{low}) and Tet-On E-cadherin^{high} (MDA-Ecad^{high}) cells.

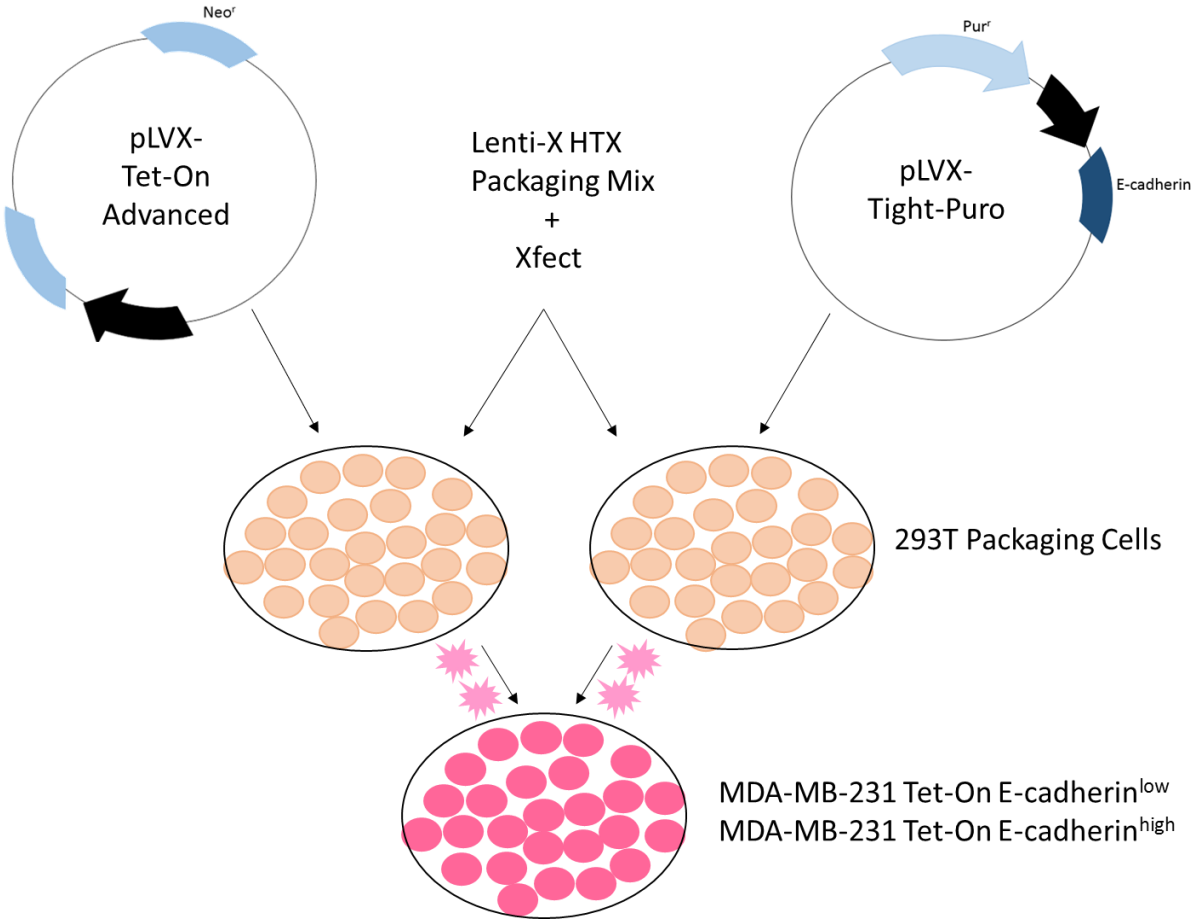
Neo^r
pLVX-
Tet-On
Advanced
Lenti-X HTX
Packaging Mix
+
Xfect
Pur^r
pLVX-
Tight-Puro
E-cadherin
293T Packaging Cells
MDA-MB-231 Tet-On E-cadherin^{low}
MDA-MB-231 Tet-On E-cadherin^{high}

Figure 5. E-cadherin levels in transfected MDA-MB-231 and MCF7 cell lines. (A) RT-qPCR showing E-cadherin transcript levels in MDA-WT, MDA-Ecad^{low}, and MDA-Ecad^{high} cells, and MCF knock-down cells. mRNA levels are normalized to GAPDH and graphed as average fold of expression ± SE when compared to the control. (B) Western blotting showing E-cadherin protein expression in MDA-Ecad^{low} and MDA-Ecad^{high} cells, as well as MCF7 knock-down cells. MDA-Ecad^{high} shows a 300% increase in E-cadherin protein levels compared to control. MCF7-si-Ecad shows an 87% decrease in E-cadherin protein levels compared to MCF-scrambled. Values for protein level changes were measured using ImageJ. E-cadherin mouse mAB was used to detect E-cadherin protein levels and α-tubulin mouse mAB was used as a loading control.

(A)

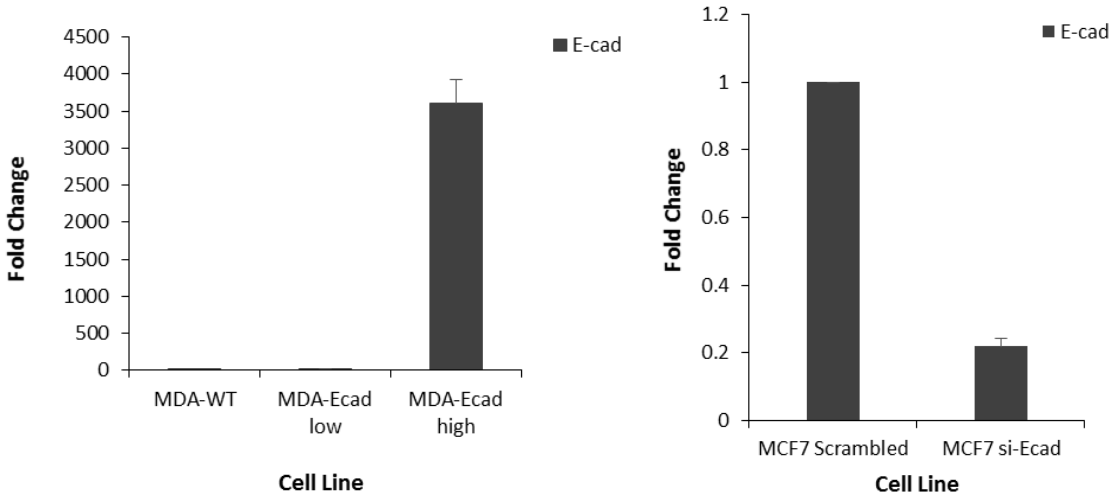
4500
4000
3500
3000
2500
2000
1500
1000
500
0
Fold Change
E-cad
MDA-WT
MDA-Ecad low
MDA-Ecad high
Cell Line
1.2
1
0.8
0.6
0.4
0.2
0
Fold Change
E-cad
MCF7 Scrambled
MCF7 si-Ecad
Cell Line

(B)

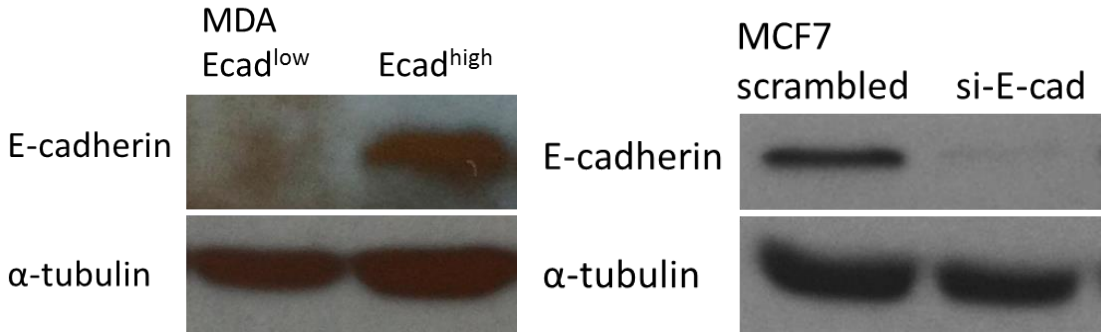
MDA
Ecad^low
Ecad^high
E-cadherin
α-tubulin
MCF7
scrambled
si-E-cad
E-cadherin
α-tubulin

Figure 6. Opposing effects of different Wnt inhibitors on MDA-MB-231 cells expressing high versus low levels of E-cadherin. MDA-Ecad^{low} (left panel) and MDA-Ecad^{high} (right panel) treated with vehicle for 4 days (first row); 5 μM p300/β-catenin inhibitor IQ-1 (second row) 5 μM CBP/β-catenin inhibitor ICG-001 (third row); 5 μM TCF4 inhibitor BC21 (fourth row). Images were taken at 5x magnification and bar represents 200 μm.

MDA-Ecad^{low} MDA-Ecad^{high}

Vehicle Control

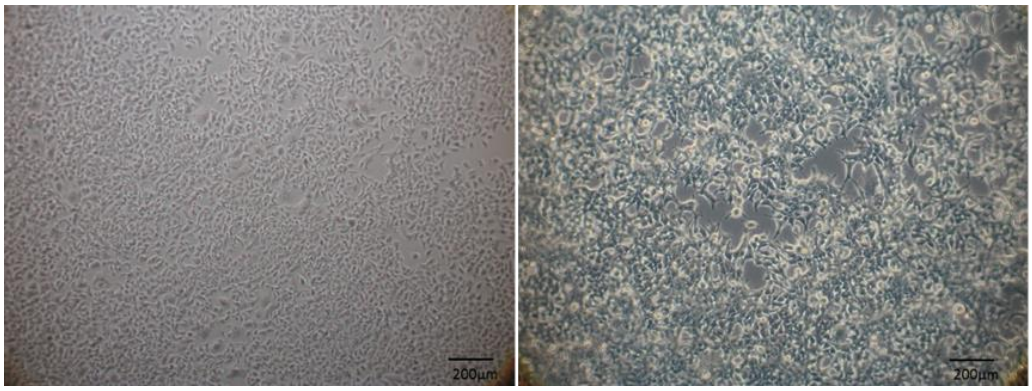

5 µM IQ-1

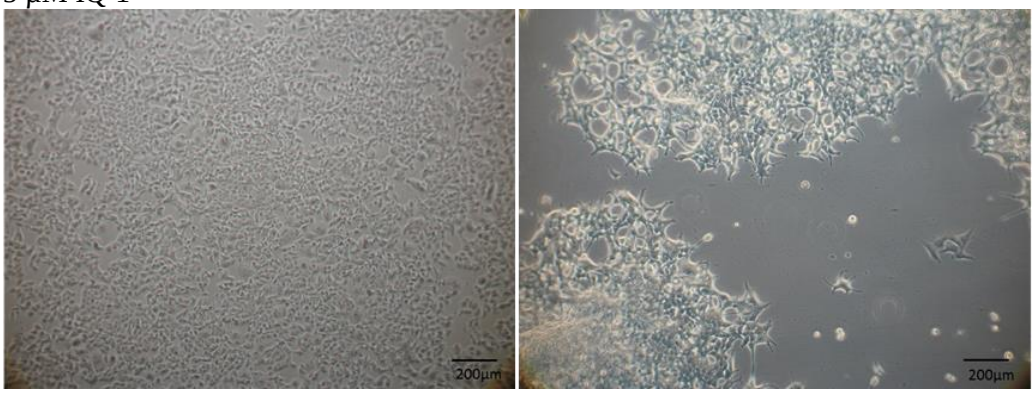

10 µM ICG-001

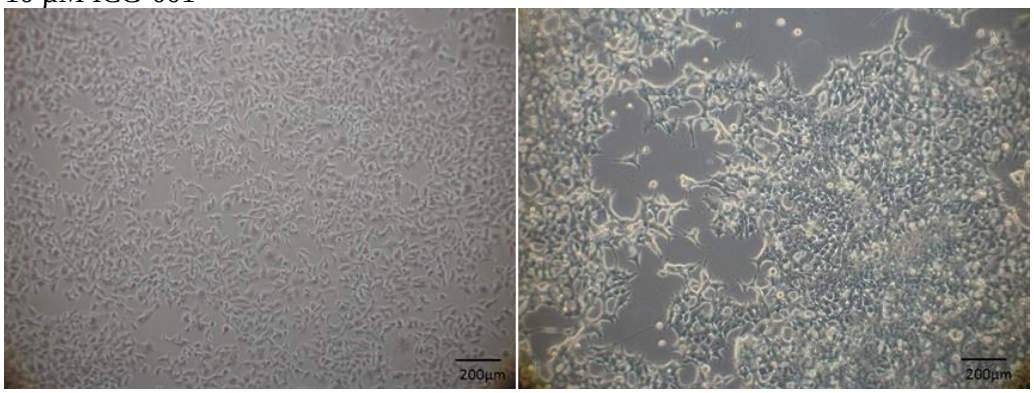

5 µM BC21

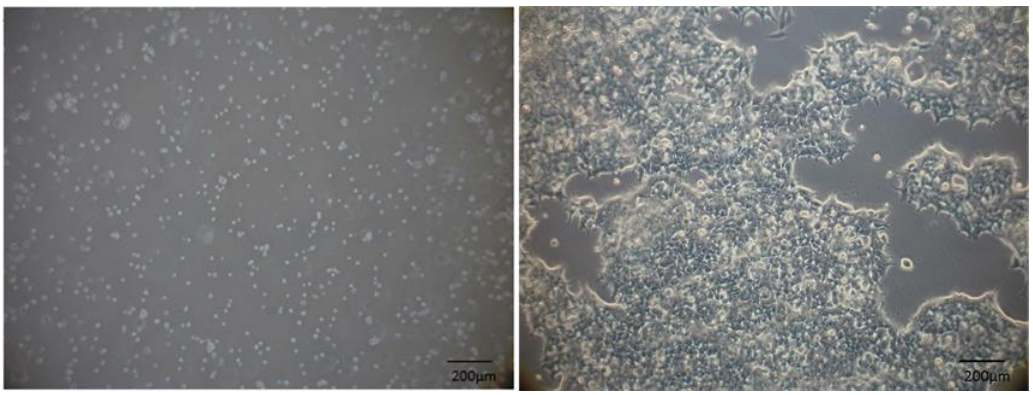

3.2 E-cadherin high cells are more resistant to TCF4 inhibitor BC21 than are E-cadherin low cells.

To validate the initial results observed with TCF4 inhibition, cells were treated with 5 μM BC21 or vehicle control for 4 days and harvested on day 5. MDA-Ecad^{low} cells showed a robust decrease in live cells compared to vehicle control when counted with trypan blue staining, whereas MDA-Ecad^{high} cells only had a slight decrease in live cell numbers (Figure 7A). Results were confirmed with an MTT assay measuring metabolic activity (Figure 7B). A similar pattern to MDA-Ecad^{high} was seen in MCF7 wild-type cells treated with 5 μM BC21 (Figure 7A and B), however knock-down conditions showed only a slight decrease in MCF7-si-E-cad cell numbers compared to MCF7-scrambled (data not shown). In addition, MDA-Ecad^{high} cells were treated with BC21 every day for 12 days to confirm that cells were able to survive and proliferate passed the standard 4 day treatment (Figure 7C). After initial cell death and slowed proliferation, cells were able to recover back to typical growth rates.

Figure 7. E-cadherin expression increases resistance to Wnt/TCF4 inhibitors. E-cadherin low cells are more susceptible to cell death induced by TCF4 inhibition than are E-cadherin high cells as shown by trypan blue staining (A) and MTT assays (B). Similar results are obtained when MCF7 cells (expressing high levels of E-cadherin) are treated with TCF4 inhibitor BC21. (C) MDA-Ecad^{high} cells recover and continuously proliferate after initial treatment with 5 μM BC21. Bar graph represents average cell count ± SE (trypan blue) or percentage of live cells ± SE as compared to vehicle control (MTT). Results are considered significant when $p < 0.05$.

(A)

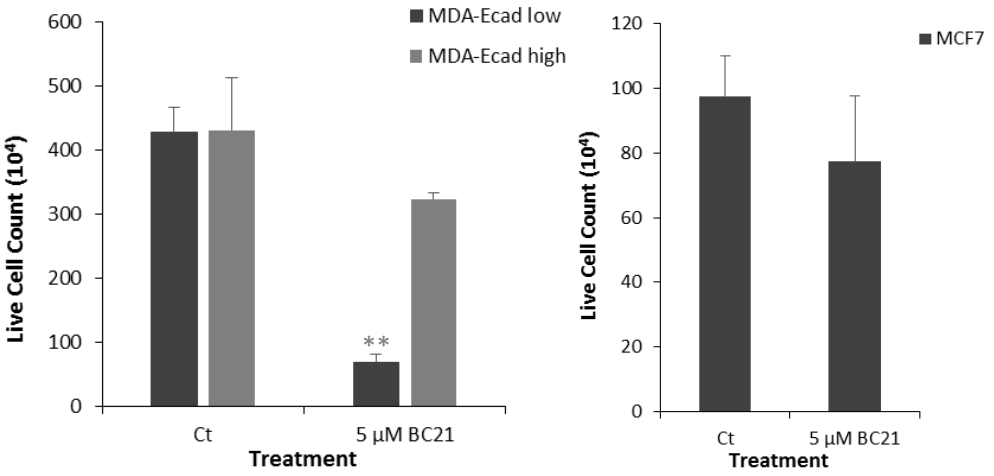
MDA-Ecad low
MDA-Ecad high
Live Cell Count (10^4)
600
500
400
300
200
100
0
**
Ct
5 µM BC21
Treatment
MCF7
Live Cell Count (10^4)
120
100
80
60
40
20
0
Ct
5 µM BC21
Treatment

(B)

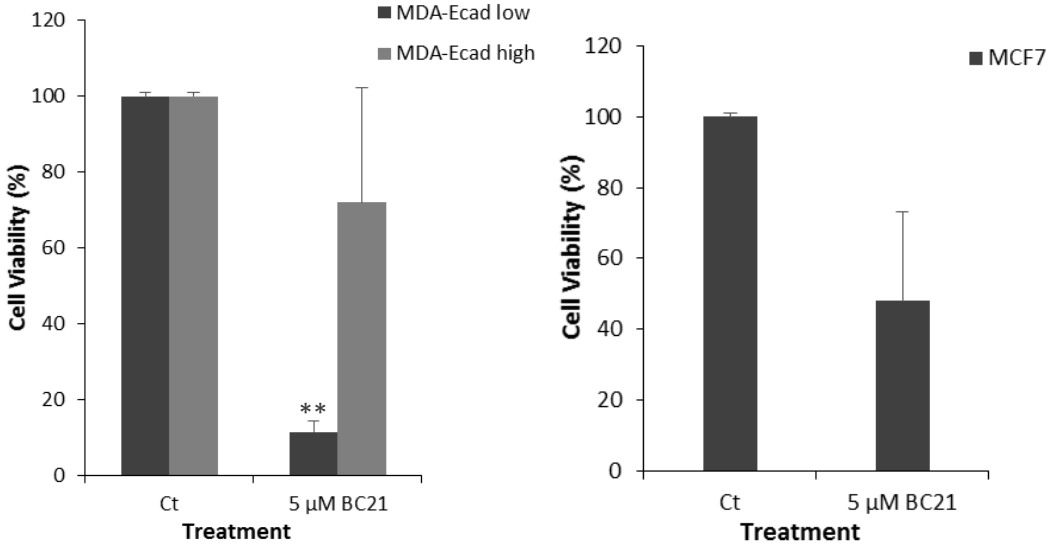
MDA-Ecad low
MDA-Ecad high
Cell Viability (%)
120
100
80
60
40
20
0
**
Ct
5 µM BC21
Treatment
MCF7
Cell Viability (%)
120
100
80
60
40
20
0
Ct
5 µM BC21
Treatment

(C)

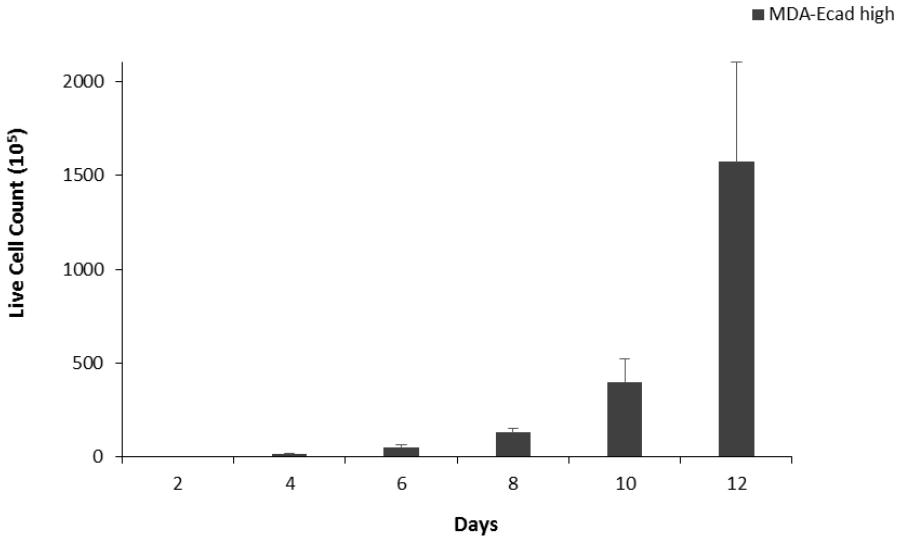
MDA-Ecad high
Live Cell Count (10^5)
2000
1500
1000
500
0
2
4
6
8
10
12
Days

3.3 Cell death in MDA-Ecad^{low} cells caused by Wnt inhibitor is associated with apoptosis.

The mechanism of cell death for MDA-Ecad^{low} cells was determined using various apoptotic markers. Transcript levels for p21, a cyclin-dependent kinase inhibitor that prevents progression at the G_1 and S phase, were increased 2.5-fold in MDA-Ecad^{low} cells treated with 5 μM BC21 (Figure 8A). Similarly, transcript levels for caspase-3, a protein that plays a central role in the execution of apoptosis, were increased 70-fold in treated cells (Figure 8A). PARP detects single-strand DNA breaks from metabolic, chemical or radiation-induced damage and signals for repair. When damage is too severe, PARP is cleaved by caspase-3 during programmed cellular death to prevent ATP depletion. Cleaved PARP protein levels increased in BC21 MDA-Ecad^{low} cells compared to control, indicating programmed cell death (Figure 8B). Lastly, Annexin V staining in flow cytometry detects cells that express phosphatidylserine on the cell surface, an event seen in apoptosis and other forms of cell death. 7-AAD is a fluorescent intercalator that has a strong affinity for DNA and undergoes a spectral shift upon association. Thus, 7-AAD is generally excluded from live cells and acts as a viability stain. When MDA-Ecad^{low} cells were stained with Annexin V and 7-AAD, half of the BC21 treated population stained positive for Annexin V/7-AAD or 7-AAD alone (Figure 8C). The mean frequency of cells stained positive for Annexin V/7-AAD or 7-AAD alone is 4.39% in control cells and 20.8% in cells treated with 5 μM BC21.

Figure 8. TCF4 inhibitor BC21 causes MDA-Ecad^{low} cells to undergo apoptosis. (A) RT-qPCR of p21 (associated with cell cycle arrest) and caspase-3 (downstream effector protein in cell death, including apoptosis) genes in MDA-Ecad^{low} cells treated with 5 μM BC21. mRNA levels are normalized to GAPDH and graphed as average fold of expression when compared to the control. (B) Western blot of PARP (left panel). Increased cleavage of PARP (PARP-C) in MDA-Ecad^{low} cells treated with 5 μM BC21 suggest activated caspase enzymes associated with apoptosis. PARP rabbit mAb was used to detect total levels of PARP (PARP-T), PARP cleaved at Asp 214 rabbit mAb was used to detect PARP-C, and α-tubulin mouse mAb was used as a loading control. ImageJ was used to measure the density of the Western blot bands, which were then normalized to α-tubulin (right panel). (C) Flow cytometry showing an increased number of BC21 treated cells stained positive for both Annexin V and 7-AAD, indicating increased cell death through apoptosis. Results are considered significant when $p < 0.05$.

(A)

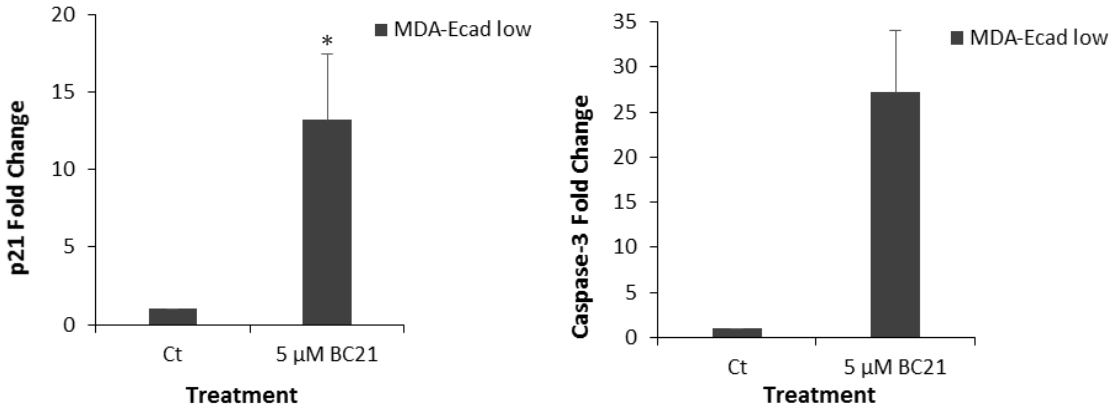
MDA-Ecad low
p21 Fold Change
20
15
10
5
0
*
Ct
5 µM BC21
Treatment
MDA-Ecad low
Caspase-3 Fold Change
35
30
25
20
15
10
5
0
Ct
5 µM BC21
Treatment

(B)

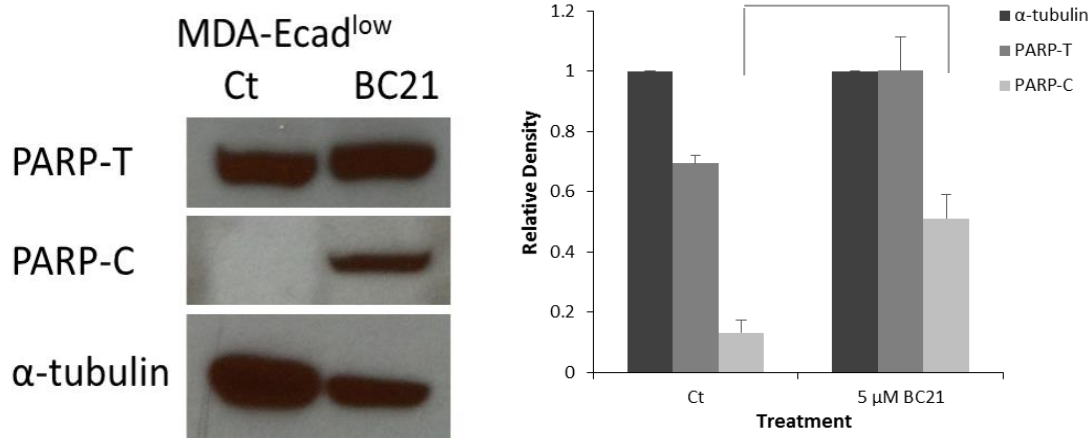
MDA-Ecad^low
Ct
BC21
PARP-T
PARP-C
α-tubulin
*
α-tubulin
PARP-T
PARP-C
Relative Density
1.2
1
0.8
0.6
0.4
0.2
0
Ct
5 µM BC21
Treatment

(C)

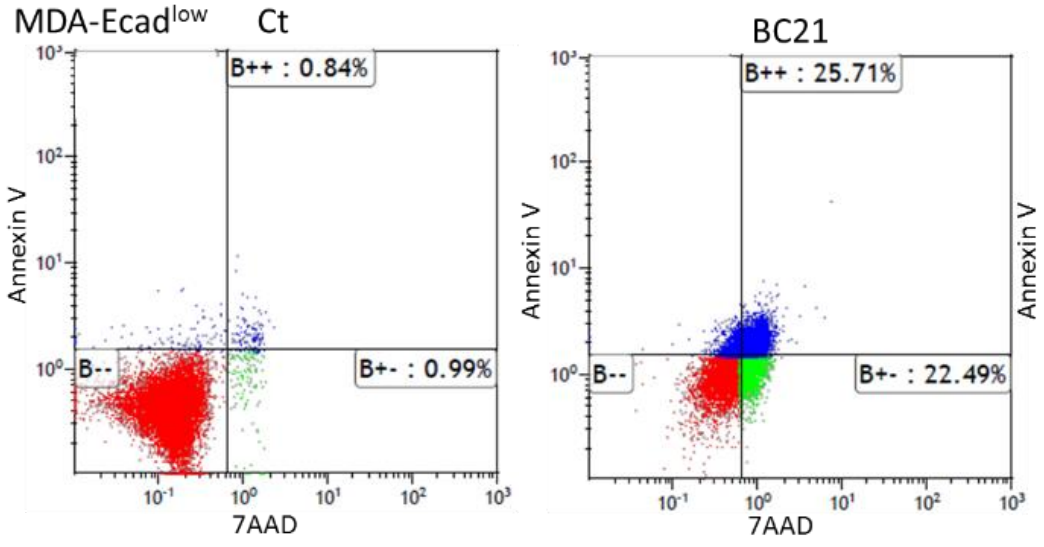
MDA-Ecad^low
Ct
B++ : 0.84%
B+- : 0.99%
B--
Annexin V
7AAD
BC21
B++ : 25.71%
B+- : 22.49%
B--
Annexin V
7AAD

3.4 High E-cadherin in combination with Wnt targeting drugs enhances phenotypes associated with breast CSCs.

Similar to induced pluripotent stem cells (iPSCs), cancer stem cells show increased expression of a core set of transcription factors (Oct3/4, Klf4, Sox2, c-Myc). These transcription factors are responsible for the stem cell-like characteristics seen in CSCs, including self-renewal and proliferation (105–107). Therefore, a western blot was used to determine whether the surviving cells in the MDA-Ecad^{high} population expressed higher levels of these core transcription factors (Figure 9A). Indeed, MDA-Ecad^{high} cells treated with 5 µM BC21 for 4 days showed increased protein expression for c-Myc, Oct3/4, and Klf4 compared to vehicle control. To confirm that BC21 induces a CSC phenotype in MDA-Ecad^{high}, cells were analyzed with flow cytometry to determine if treated cells showed an increased CD44^{high}/CD24^{low} profile. CD44 is a class I transmembrane glycoprotein that is critical in regulating stem cell-like characteristics, such as proliferation, growth, survival, migration, and angiogenesis. Alternatively, CD24 is a glycoprotein that is anchored to the cell surface by glycosyl-phosphotidyl-inositol and is associated with a differentiated epithelial phenotype. Flow cytometry of E-cadherin high cells revealed a distinct population of cells with a CD44^{high}/CD24^{low} profile, which was increased after BC21 treatment (Figure 9B). The mean frequency of cells stained positive for CD44^{high}/CD24^{low} is 1.64% in control cells and 3.19% in cells treated with 5 µM BC21. These results are considered significant ($p < 0.05$) and further suggests the up-regulation of a CSC population as indicated with western blotting

Figure 9. TCF4 inhibition promotes a CSC phenotype in E-cadherin high cells. (A) Western blot analysis of cancer-promoting proteins in MDA-Ecad^{high} cells treated with 5 μM BC21 (left panel). c-Myc rabbit mAb, Oct3/4 rabbit pAb and Klf4 rabbit pAb were used to detect protein levels and were compared to α-tubulin mouse mAb as a loading control. ImageJ was used to measure the density of the Western blot bands, which were then normalized to α-tubulin (right panel). Results are considered significant when $p < 0.05$. (B) Flow cytometry analysis showing an increased CD44+/CD24- profile in MDA-Ecad^{high} treated cells.

(A)

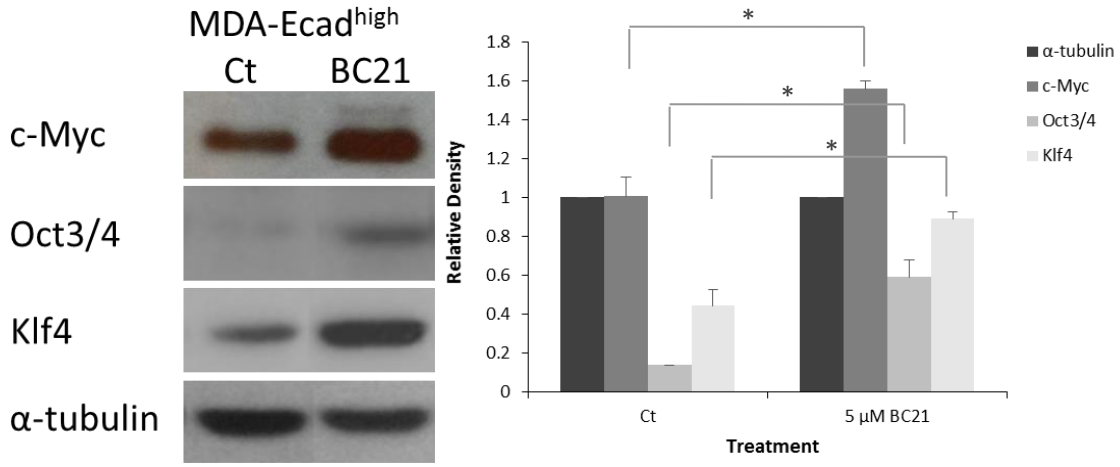
MDA-Ecad^high
Ct
BC21
c-Myc
Oct3/4
Klf4
α-tubulin
Relative Density
1.8
1.6
1.4
1.2
1
0.8
0.6
0.4
0.2
0
*
*
*
Ct
5 μM BC21
Treatment
α-tubulin
c-Myc
Oct3/4
Klf4

(B)

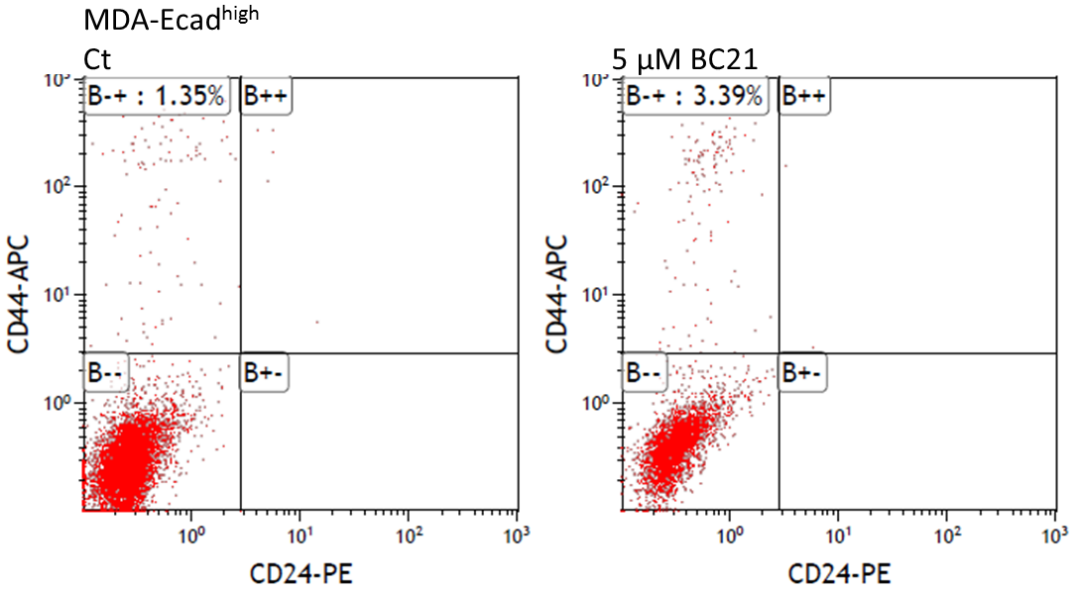
MDA-Ecad^high
Ct
B-+ : 1.35%
B++
B--
B+-
CD44-APC
CD24-PE
5 μM BC21
B-+ : 3.39%
B++
B--
B+-
CD44-APC
CD24-PE

3.5 Additional activation of Wnt by GSK-3 inhibitor BIO, further enhances effects seen with BC21.

As previously mentioned, GSK-3 functions as an inhibitor of the Wnt pathway through its role in the destruction complex for cytoplasmic β-catenin. To account for fluctuating levels of Wnt signalling in living systems, 2.5 μM of GSK-3 inhibitor BIO was added daily to cell cultures to mimic increased Wnt activation. BIO alone caused minimal cell death (Figure 10B), however, when added with 5 μM BC21 robust cell death was seen only in MDA-Ecad^{low} cells and survival was 3x lower than BC21 alone (Figure 10A and B). MDA-Ecad^{high} cells, on the other hand, displayed no significant cell death when counted with trypan blue (Figure 10B) and formed clustered spheres in culture (Figure 10A). When MDA-Ecad^{low} cells were analyzed for cell death, 95% of the cells treated with CHIR-99021 (an alternative GSK-3 inhibitor) and BC21 were stained positive for Annexin V/7-AAD or 7-AAD alone, compared to 1% treated with CHIR-99021 alone or 50% with BC21 alone (Figure 10C). The mean frequency of cells stained positive for Annexin V/7-AAD or 7-AAD alone is 4.38% in control cells, 20.8% in cells treated with 5 μM BC21, and 60% in cells treated with 5 μM CHIR and 5 μM BC21. (Note: CHIR-99021 replaced BIO during flow cytometry experiments due to fluorescent interference.)

The propensity for MDA-Ecad^{high} cells to form spherical cultures was investigated by colony formation assays, which measures the ability of a single cell to grow anchorage-independently and to give rise to a colony, an indicator of CSC properties (108, 109). Only spheres that exceeded 100 μm in diameter and stained positive with MTT (live cells) were considered to be colonies (Figure 11A) (110, 111). For all treatment conditions, there was a

decrease in colony numbers for MDA-Ecad^{low} cells, compared to vehicle control (Figure 11B). Conversely, both BIO alone and BIO + BC21 treatments led to an increase in clonogenic capacity in MDA-Ecad^{high} cells, with BIO + BC21 having the highest colony numbers and largest spheres (Figure 11A and B).

Figure 10. Addition of GSK-3 inhibitor BIO with BC21 treatment enhances cell death in MDA-Ecad^{low} cells without significant effect in MDA-Ecad^{high} cells. (A) MDA-Ecad^{low} cells treated with 2.5 µM BIO + 5 µM BC21 for 4 days (left); MDA-Ecad^{high} cells treated with 2.5 µM BIO + 5 µM BC21 for 4 days (right). Images were taken at 5x magnification and bar represents 200 µm. (B) Live cell count using trypan blue staining on MDA-Ecad^{low} and MDA-Ecad^{high} cells with 2.5 µM BIO and/or 5 µM BC21 for 4 days. Bar graph represents average cell count ± SE and results are considered significant when $p < 0.05$. (C) Flow cytometry showing a further increase in apoptotic cells in MDA-Ecad^{low} with the addition of 5 µM CHIR-99021 (replacement for BIO) to 5 µM BC21. Patterned bars (▨) indicate data previously shown.

(A)

2.5 μM BIO + 5 μM BC21

MDA-Ecad^{low} MDA-Ecad^{high}

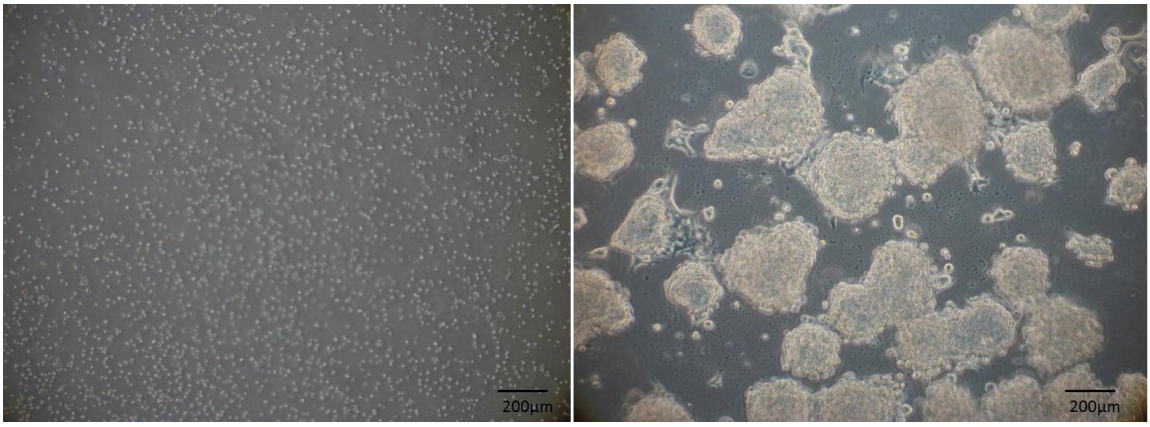

(B)

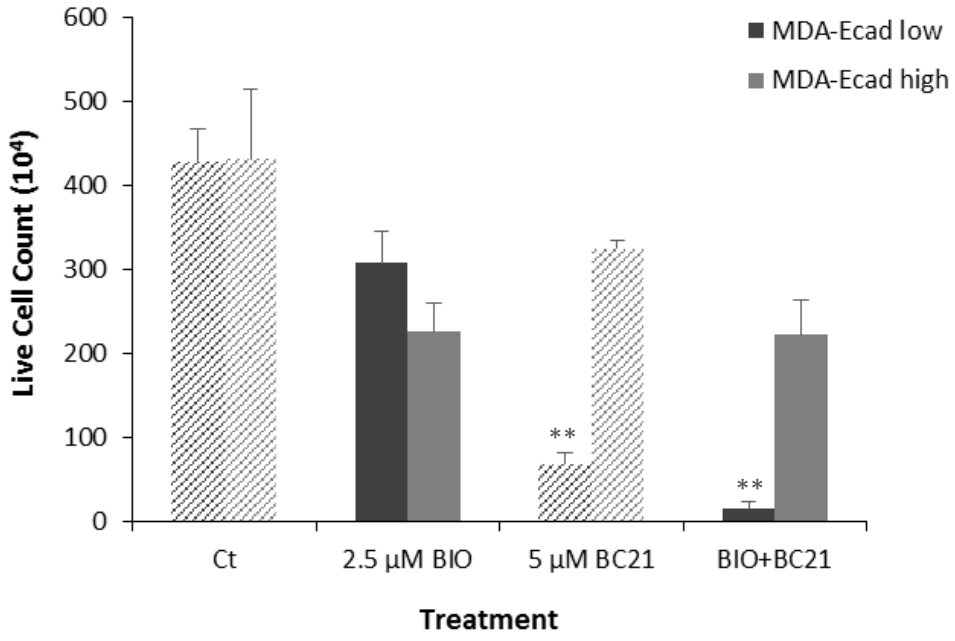

(C)

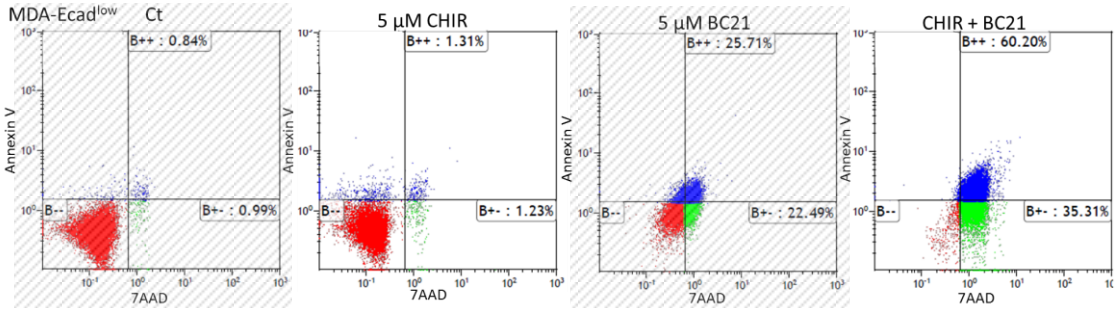

Figure 11. Activation of Wnt using BIO enhances physical CSC characteristics when combined with BC21. (A) Depiction of a 21 day colony formation assay in MDA-Ecad^{high} cells with vehicle control (top left); 2.5 µM BIO (top right); 5 µM BC21 (bottom left); 2.5 µM BIO + 5 µM BC21 (bottom right). Cell viability in colonies was determined by positive MTT staining (dark blue). Images were taken at 5x magnification and bar represents 200 µm. (B) Count of spheres (≥100 µm) from colony formation assays initially treated with 2.5 µM BIO and/or 5 µM BC21. Bar graph represents average sphere count ± SE of live cells as indicated through MTT staining. Results are considered significant when $p < 0.05$.

(A)

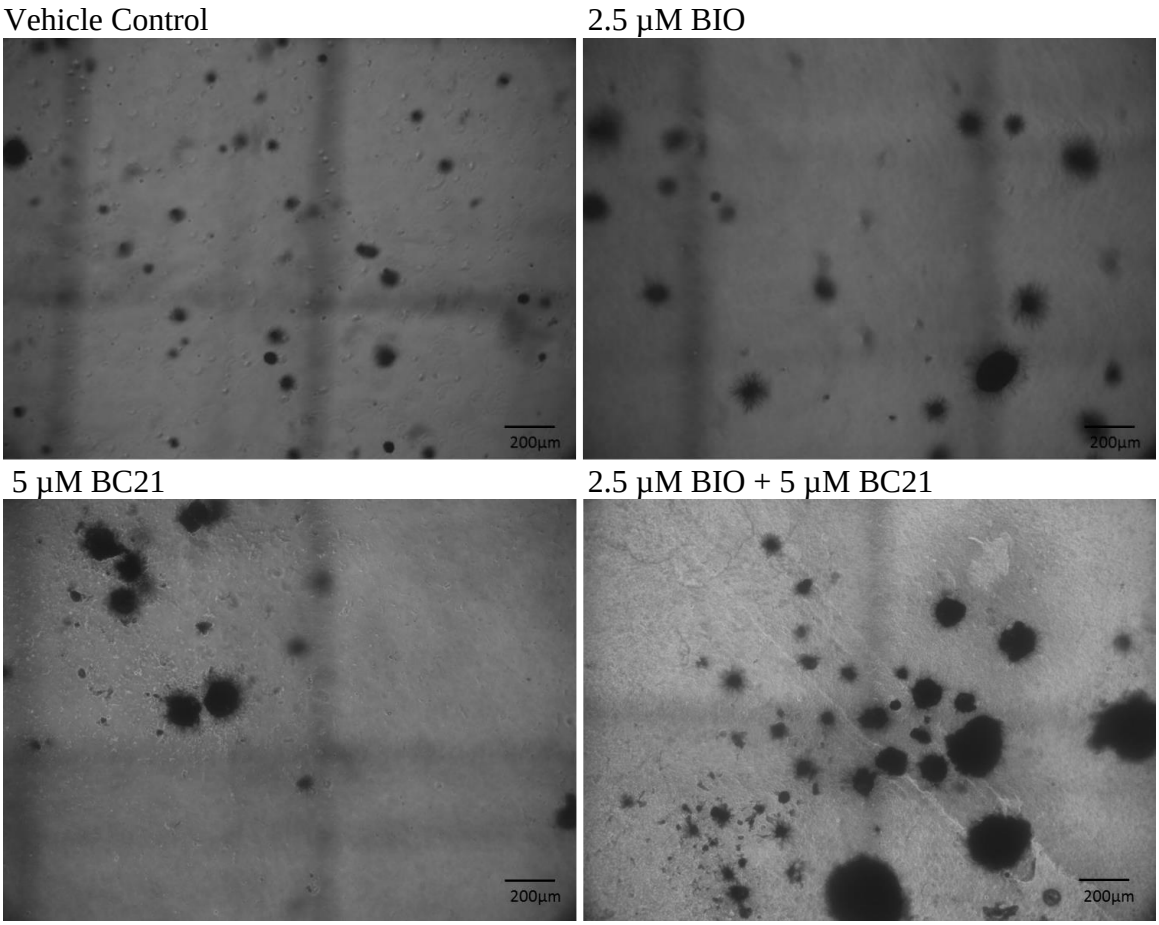
Vehicle Control
2.5 µM BIO
5 µM BC21
2.5 µM BIO + 5 µM BC21
200µm
200µm
200µm
200µm

(B)

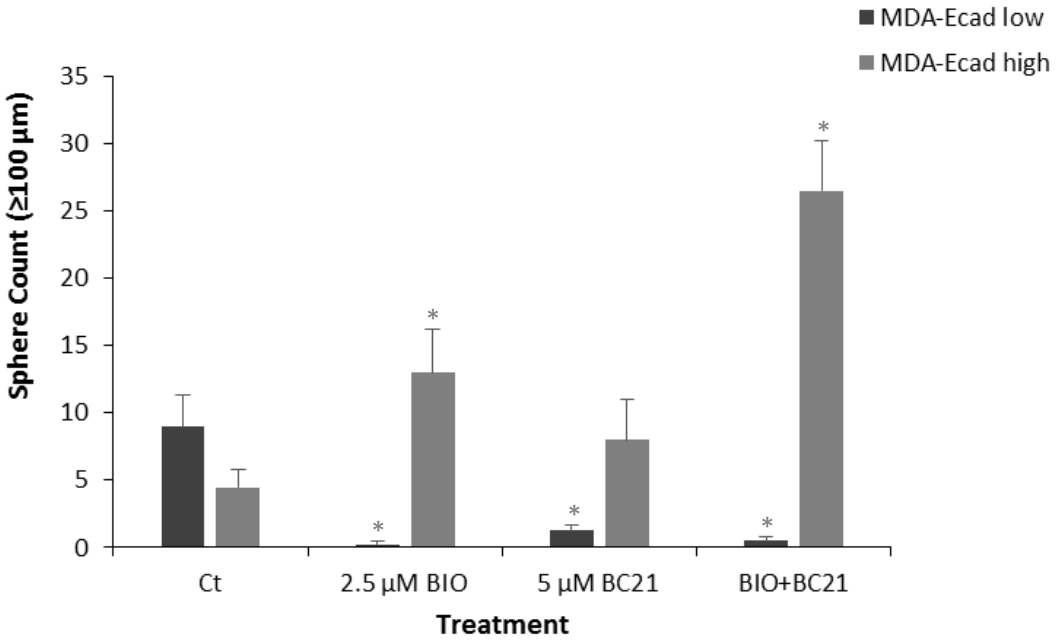
MDA-Ecad low
MDA-Ecad high
Sphere Count (≥100 µm)
35
30
25
20
15
10
5
0
*
*
*
*
Ct
2.5 µM BIO
5 µM BC21
BIO+BC21
Treatment

3.6 E-cadherin high cells express increased levels of activated Akt, and therefore blockage of Akt is needed to effectively arrest the growth of breast cancer cells expressing high levels of E-cadherin.

Given that Wnt inhibitors are ineffective against cells with high levels of E-cadherin, I explored the possibility that another major pathway was activated in E-cadherin high breast cancer cells. Previous research has indicated that high levels of E-cadherin enhance PI3K signalling, therefore I tested MDA-Tet-On cells for differential Akt activation, a protein kinase downstream of PI3K. Indeed, MDA-Ecad^{high} cells showed increased phosphorylated Akt (Akt-P) compared to MDA-Ecad^{low} cells (Figure 12A), indicating activated Akt correlates with high E-cadherin expression. MDA-Ecad^{low}, MDA-Ecad^{high}, and MCF7 were then treated with 3 μM Akt VIII inhibitor for 4 days. There was significantly more cell death, as measured with trypan blue staining and MTT viability assays, in MDA-Ecad^{high} and MCF7 cells, whereas MDA-Ecad^{low} cells were largely unaffected (Figure 12B and C). Again, there was very little difference between MFC7-scrambled and MCF7-si-Ecad (data not shown).

Figure 12. Blockage of Akt enhances cell death in cells previously unaffected by TCF4 inhibition. (A) Western blot analysis of activated Akt (Akt-P) in MDA-MB-231 cells (left panel). Total Akt was detected using Akt rabbit mAb, activated Akt was detected using Akt-phospho on Ser473 rabbit mAb, and results were compared to α-tubulin mouse mAb as a loading control. ImageJ was used to measure the density of the Western blot bands, which were then normalized to α-tubulin (right panel). Cell count using trypan blue staining (B) and cell viability using MTT (C) on MDA-Ecad^{high}, MDA-Ecad^{low}, and MCF7 cells treated with 3 μM Akt VIII inhibitor. Bar graph represents average cell count ± SE (trypan blue) or percentage of live cells ± SE as compared to vehicle control (MTT). Results are considered significant when $p < 0.05$.

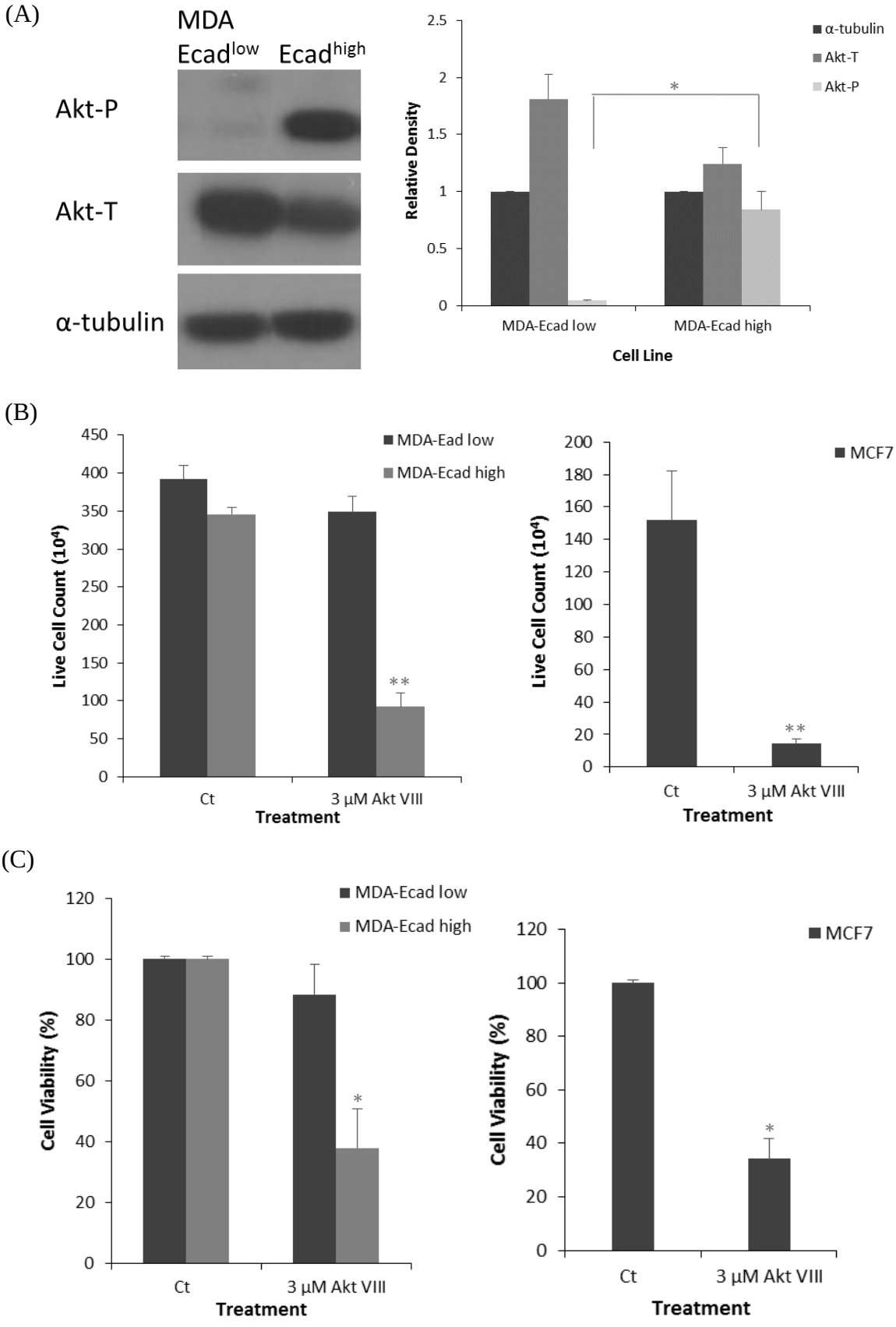
(A)
MDA
Ecad^low
Ecad^high
Akt-P
Akt-T
α-tubulin
Relative Density
α-tubulin
Akt-T
Akt-P
MDA-Ecad low
MDA-Ecad high
Cell Line
(B)
MDA-Ead low
MDA-Ecad high
Live Cell Count (10^4)
Ct
3 µM Akt VIII
Treatment
MCF7
(C)
MDA-Ecad low
MDA-Ecad high
Cell Viability (%)
MCF7

4. DISCUSSION

E-cadherin is a major cell-cell contact adhesion molecule, and for the most part, it has been implicated as a tumour suppressor in various human epithelial tumours. However, there are an increasing number of studies that indicate a promoting role for E-cadherin in tumour progression (56–58, 112–114). In accordance with this data, my current study indicates that fluctuating levels of E-cadherin, indicative of EMT/MET interconversion, alters the signalling profile of breast cancer cells, resulting in changes to therapeutic susceptibility.

4.1 Establishing the influence of E-cadherin levels on Wnt signalling

MDA-MB-231 breast cancer cells normally express very low levels of endogenous E-cadherin, and are accordingly classified as an invasive, mesenchymal cell line. Overexpression of E-cadherin in this cell line, as introduced through a lentiviral Tet-On system, led to a more drastic spindle-like morphology and increased proliferation, as observed through a light microscope (data not shown). To determine if the differences between the low and high E-cadherin cell lines extended beyond observable changes, MDA-Tet-On cells were treated with various Wnt inhibitors. The canonical Wnt signalling pathway has been extensively researched in cancer progression, however, due to its numerous interactions and differential outcomes during activation, it is unclear whether Wnt will promote or inhibit tumour progression in a given cell type. The role of Wnt signalling in breast cancer was assessed in MDA-MB-231 cells using inhibitors that targeted β-catenin's interaction with transcription factors p300 (IQ-1), CBP (ICG-001), and TCF4 (BC21). Whereas IQ-1 was largely ineffective in bringing about cellular changes (data not shown),

ICG-001 (data not shown) and BC21 treatments resulted in cell death only in MDA-Ecad^{low} cells, with greater disparity between MDA-Ecad^{low} and MDA-Ecad^{high} cell survival with BC21 treatments (Figure 7A and B). Although these inhibitors all target the Wnt pathway, differing outcomes indicate that CBP and TCF4 are more heavily involved in the transcription process than are other transcription factors, such as p300, due to efficacy of inhibitors or biological response of cells. This conclusion is partly explained by a model proposed by Teo and Kahn, which states that the divergent activities of Wnt signalling can be attributed to the coactivators CBP and p300 (115). Their model explains that CBP/β-catenin mediated transcription is critical for stem cell/progenitor cell maintenance and proliferation, whereas p300/β-catenin initiates differentiation. Since MDA-MB-231 cells are an aggressive, mesenchymal cell type, my research coincides with the model in that these cells emphasize CBP. On a similar note, the transcription factor TCF4 has been shown to promote cancer initiation and progression when associated with β-catenin, while exhibiting a tumour suppressor function when the Wnt pathway is inactive (116–119). Focus was placed on TCF4 inhibitor BC21 because of its controversial role in promoting or inhibiting breast cancer. Treatments with this inhibitor resulted in the largest disparity between MDA-Ecad^{low} and MDA-Ecad^{high} cells, and further research into the reason behind this discrepancy could explain TCF4's role as both a tumour promoter and repressor.

4.2 Does cell death resulting from TCF4 inhibition in E-cadherin low cells occur through apoptosis?

When under severe stress, cells may undergo programmed cell death, such as apoptosis, or non-physiological cell death, such as necrosis. During apoptosis, death factors bind to tumour necrosis factor receptors that result in a signalling cascade leading to the activation of initiator caspases (2, 8 – 12) that proteolytically cleave effector caspases (3, 6, 7). Effector caspases carry out apoptosis through degradation of intracellular proteins (120, 121). Necrosis occurs as a result of infection, toxins, or trauma that leads to ruptures in the cell membrane and release of its contents. The inflammatory response that ensues prevents phagocytosis and the environment becomes toxic to surrounding healthy tissue (122, 123). Transcript levels in MDA-Ecad^{low} cells treated with BC21 showed a 2.5-fold increase in p21, a cyclin-dependent kinase inhibitor that regulates cell cycle progression at the G_1 and S phase, and a 70-fold increase in caspase-3, compared to vehicle control (Figure 8A). Similarly, western blots detected cleaved PARP in treated MDA-Ecad^{low} cells, but not in control (Figure 8B). Lastly, flow cytometry analysis revealed a 26% increase in Annexin V$^+$/7-AAD$^+$ and a 22% increase in 7-AAD$^+$ populations in MDA-Ecad^{low} cells treated with BC21 (Figure 8C). As previously mentioned, Annexin V is used to detect cells expressing phosphatidylserine on their surface, an event seen during apoptosis, and 7-AAD is used as a viability stain. Taken together, these results indicate that cell death in MDA-Ecad^{low} cells treated with BC21 is due to programmed cell death, specifically apoptosis, and is not a result of necrotic death.

4.3 Enhanced CSC characteristics seen in E-cadherin high cells through Wnt inhibition

Unlike MDA-Ecad^{low} cells, BC21 had little to no effect on MDA-Ecad^{high} cells. Indeed, MDA-Ecad^{high} cells were able to recover and continue to proliferate alongside constant BC21 treatment (Figure 7C). One characteristic of cancer stem cells is resistance to traditional chemotherapeutic drugs, allowing for recolonization of a tumour population. Pioneering research by Takahashi and Yamanaka first revealed what we now refer to as the "core transcription factors" that confer stemness and can be used in to reprogram epithelial cells into iPSCs (105). To determine if treatment with BC21 leads to a CSC phenotype, and in turn, confers BC21 resistance in MDA-Ecad^{high} cells, cells were treated with 5 μM BC21 for 4 days and analyzed with western blot (Figure 9A) and flow cytometry (Figure 9B). Western blot reveals a 2-3 fold increase in c-Myc, Oct4 and Klf4 protein levels and flow cytometry shows a 2% increase in $CD44^{+}/CD24^{-}$ cell populations in MDA-Ecad^{high} treated with BC21 compared to vehicle control. $CD44^{+}/CD24^{-}$ cell surface proteins are common markers used in breast cancer to distinguish potential CSC populations. Taken together, these results indicate an increased CSC population in MDA-Ecad^{high} cells after treatment with BC21.

Just as E-cadherin levels in a given cell are not constant, activation or inhibition of a particular pathway will vary in order to adapt to changing environmental conditions. Therefore, to determine if further activation of Wnt signalling, which is often seen in breast cancer cells, would enhance cellular effects already seen, cells were treated with GSK-3 inhibitor BIO, theoretically leading to an increase in free β-catenin available in the cytoplasm and allowing for interaction with E-cadherins at the membrane or transportation into the nucleus to activate transcription. BIO and BC21 treatment led to almost complete cell death

in MDA-Ecad^{low}, as indicated by trypan blue counting (Figure 10B) and flow cytometry analysis with Annexin V and 7-AAD (Figure 10C). Conversely, BIO and BC21 treatment resulted in MDA-Ecad^{high} cells forming sphere-like structures in standard cell culture conditions (Figure 10A). A colony formation assay confirmed that treatment of MDA-Ecad^{high} cells with both BIO and BC21 significantly increased the number (Figure 11B) and size (data not shown) of tumorspheres in culture. I hypothesize that E-cadherin low cells, the cell rely heavily on Wnt signalling through TCF4, and consequently, an increase in the amount of β-catenin available for transcription through GSK-3 inhibition will lead to a more detrimental effect when BC21 is used to inhibit TCF4. BIO at 2.5 μM is not toxic to cells when treated alone. In contrast, E-cadherin high cells are resistant to cell death with BC21 and additionally show CSC characteristics when BIO and BC21 inhibitors are combined. In this manner, BIO and BC21 work synergistically. Previous research into TCF4 and its apparent disparity as both a tumour suppressor and promoter, somewhat accounts for what I have seen with BC21 in MDA-Ecad^{low} versus MDA-Ecad^{high} cells. In E-cadherin low cells, Wnt is active causing TCF4 to theoretically act as a tumour promoter and therefore inhibition of TCF4 leads to widespread cell death. Conversely, in E-cadherin high cells, Wnt is inactive causing TCF4 to act as a tumour suppressor and inhibition by BC21 leads to tumour progression. Inhibition of GSK-3 with BIO also supports this theory, as it allows for increased β-catenin/TCF4 interaction to carry out transcription and promote carcinogenesis. However, if this were completely true, addition of BIO and BC21 would mitigate this effect, and I should see either no effect compared to vehicle control, an up-regulation of CSC characteristics that is not as robust as BIO alone, or an increase in cell death that is not as robust as BC21 alone in E-cadherin low cells. Since the combinational treatment of BIO and BC21 shows the greatest amount of CSC phenotypes and the least cell death, two

possibilities can be concluded; E-cadherin high cells place equal emphasis on Wnt, but less emphasis on TCF4 and instead use other transcription factors (LEF1, TCF1, TCF3), and/or E-cadherin expression induces a shift from Wnt signalling to another signalling pathway that regulates survival and CSC properties. Due to there being both cell death resistance and CSC phenotypes in MDA-Ecad^{high} cells, a combination of the above two hypotheses are likely to be in effect.

4.4 Wnt is not alone

Given the ineffectiveness of Wnt signalling inhibitors in repressing E-cadherin high breast cancer cells, I wanted to look at the possibility of another pathway being activated in E-cadherin high cells. If I could identify an alternative pathway that was activated, it could lead to a subtype-specific therapy by using a Wnt/TCF4 inhibitor to target cells with low E-cadherin (EMT) and another signalling pathway inhibitor to target cells with high E-cadherin (MET). Akt is a serine/threonine kinase that mediates downstream processes such as cell survival, growth, apoptosis, migration and angiogenesis (85–88). Not only is aberrant activation of Akt observed in many types of cancer, but E-cadherin has been shown to activate PI3K, a kinase upstream of Akt (56–58). Therefore, focus was placed on identifying whether MDA-Ecad^{high} cells expressed higher levels of activated Akt than MDA-Ecad^{low} cells. Western blot confirmed increased levels of activated Akt (Akt-P) in MDA-Ecad^{high} cells, but not MDA-Ecad^{low} (Figure 12A). I then wanted to determine whether an Akt inhibitor (Akt VIII) would be able to successfully induce cell death in E-cadherin high cells. As expected, 3 µM Akt VIII caused cell death in about 70% of the population in both MDA-Ecad^{high} cells and MCF7 cells, according to trypan blue counting (Figure 12B) and MTT assay (Figure 12C). In addition, the same concentration of Akt VIII induced little to no cell death in MDA-Ecad^{low} cells. These results further strengthen the theory that E-cadherin levels influence the primary signalling pathway in breast cancer cells, where low E-cadherin expression relies more heavily on the Wnt/TCF4 pathway and high E-cadherin expression relies mostly on the Akt pathway for cell survival (Figure 13). Further work will be needed to determine whether E-cadherin high cells also rely on Wnt, but place emphasis on transcription factors other than TCF4.

Figure 13. Proposed relationship between cellular E-cadherin levels and Wnt/Akt activation/inhibition. (A) In low E-cadherin cells, canonical Wnt signalling is the main pathway for cell survival, and therefore, targeting of this pathway using TCF4 inhibitor BC21 would be the most effective means of eliminating low E-cadherin breast cancer cells. (B) In high E-cadherin cells, less reliance is put upon Wnt signalling and more emphasis is on the Akt pathway. Targeting TCF4 is largely ineffective and increases CSC phenotypes, therefore inhibiting Akt signalling would be the most effective means of eliminating high E-cadherin breast cancer cells. ① Proposed thesis findings. ②③ Modified from Howard *et al.* 2003 Bmc Musculoskelet Disord 4:16 (84) and Vivanco and Sawyers. 2002 Nat Rev Cancer *2*:489 (88)

(A)

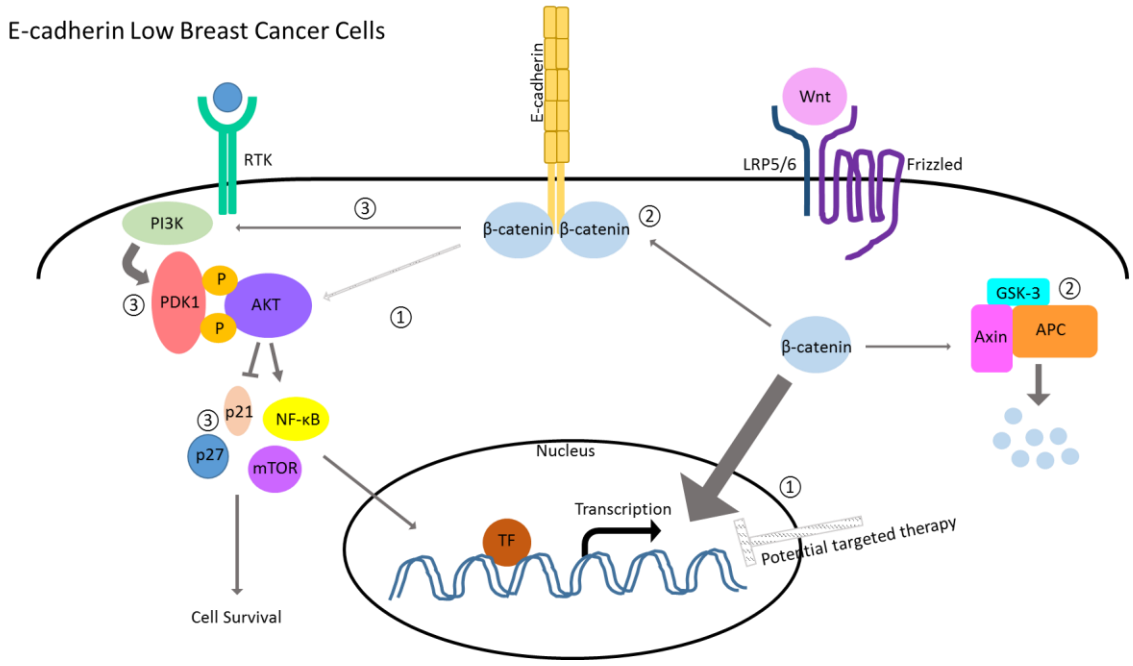
E-cadherin Low Breast Cancer Cells
E-cadherin
Wnt
RTK
LRP5/6
Frizzled
PI3K
β-catenin β-catenin
PDK1
P
AKT
P
GSK-3
Axin
APC
β-catenin
p21
NF-κB
p27
mTOR
Nucleus
Transcription
TF
Potential targeted therapy
Cell Survival

(B)

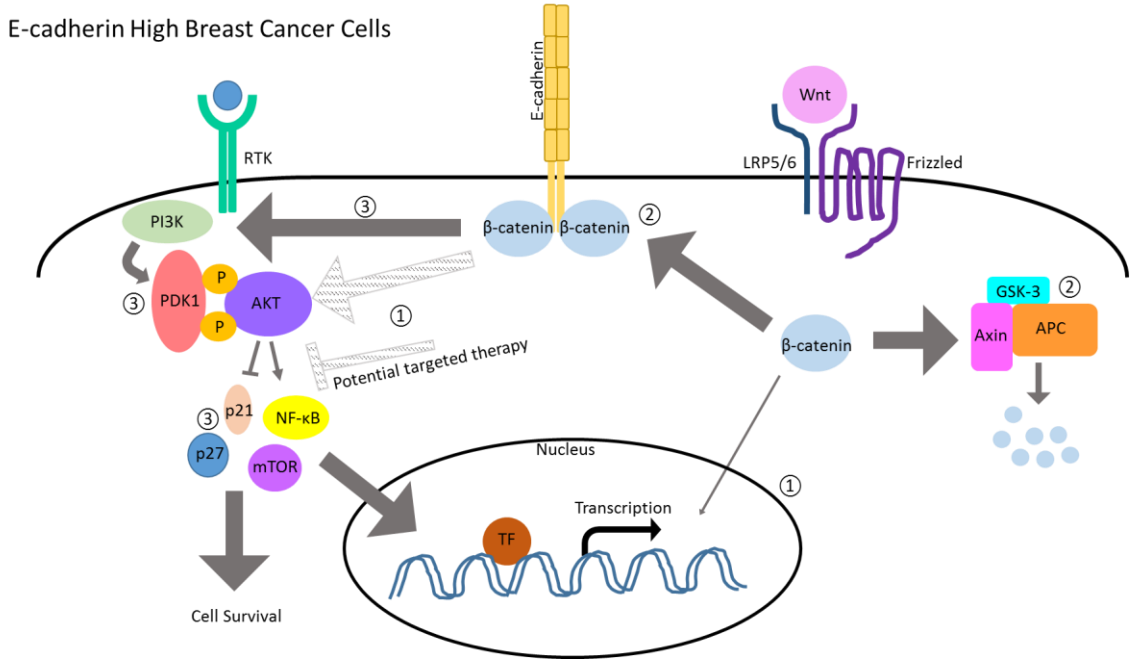
E-cadherin High Breast Cancer Cells
E-cadherin
Wnt
RTK
LRP5/6
Frizzled
PI3K
β-catenin β-catenin
PDK1
P
AKT
P
Potential targeted therapy
GSK-3
Axin
APC
β-catenin
p21
NF-κB
p27
mTOR
Nucleus
Transcription
TF
Cell Survival

4.5 Concluding remarks

Despite progress being made into the effect that E-cadherin levels have on cell survival and cancer progression, a considerable amount of research is still required to confirm this trend and to determine the exact mechanism behind it. Minor work includes finishing repeats for experiments associated with apoptosis in MDA-Ecad^{low} cells. Additionally, although a general trend similar to MDA-Ecad^{high} cells was confirmed for BC21/Akt VII treatment in MCF7 cells, which normally express high levels of E-cadherin, knock-down of MCF7 with E-cadherin siRNA yielded insignificant results, although showing a similar trend to MDA-Ecad^{low} cells. After analyzing results obtained from qPCR and western blot (Figure 5A and B), it was concluded that a knock-down efficiency of 80% was not sufficient enough to elicit global signalling changes within the cell, as baseline E-cadherin levels were still high. To solve this, our lab is looking into using CRISPR/Cas9 knock-out reagents as a more effective means of removing E-cadherin expression or repeating experiments with another breast cancer cell line that normally expresses very low to no E-cadherin within the cell (similar to MDA-MB-231 wild-type). Results regarding BC21 would also need to be confirmed with TCF4 si-RNA, to ensure that BC21 is in fact specifically targeting TCF4 and there are not any off-targets influencing the results. Next, for results to be applicable to the clinical field, treatments will be repeated using clinical samples and mouse models. Lastly, it is clear that Akt plays a significant role in either the survival or cancer progression in E-cadherin high cells treated with BC21, it is however unclear how much of a role Wnt or Akt plays and if any other signalling pathways are involved. Knock-outs and various pathway inhibitors will initially help in identifying areas of importance. In order to develop effective breast cancer

treatments, it will become imperative to determine the mechanism behind E-cadherin's influence on activating or inhibiting Wnt, Akt, and potentially other signalling pathways.

In summary, this report has shown that the susceptibility of cancer cells to therapeutic drugs relies, at least partially, on the expression level of E-cadherin. There is an increasing amount of evidence suggesting that CSCs undergo both EMT to invade from the primary tumour site into surrounding tissue and a reversion back to MET to colonize at the secondary location. My research suggests that effective eradication of CSCs will require different inhibitors targeting either the epithelial or mesenchymal state. Here, I looked at MDA-MB-231 transfected with a Tet-On expression system for either E-cadherin or vehicle control, and MCF7 breast cancer cell lines. Treatment with Wnt/TCF4 inhibitor BC21 resulted in robust cell death in low E-cadherin cells (MDA-Ecad^{low}) and little to no effect in high E-cadherin cells (MDA-Ecad^{high} and MCF7), with MDA-Ecad^{high} cells also showing a shift towards a CSC phenotype. In contrast, treatment with Akt VIII inhibitor resulted in extensive cell death in high E-cadherin cells and very little to no cell death in MDA-Ecad^{low} cells. Further research will focus on confirming these effects in both clinical samples and *in vivo* mouse models, as well as determining the mechanisms behind E-cadherin's influence on the cell's signalling pathways. Ultimately, treatment of breast cancer with a combination of BC21 and Akt VIII looks to be a promising therapeutic avenue to eradicate cancer cells and cancer stem cells, thus preventing future recurrence.

5. REFERENCES

1. 2014. World cancer report 2014. International Agency for Research in Cancer, Lyon.

2. **Cheng L, Swartz MD, Zhao H, Kapadia AS, Lai D, Rowan PJ, Buchholz TA, Giordano SH**. 2012. Hazard of Recurrence among Women after Primary Breast Cancer Treatment—A 10-Year Follow-up Using Data from SEER-Medicare. Cancer Epidemiol Biomarkers Prev **21**:800–809.

3. **Li X, Lewis MT, Huang J, Gutierrez C, Osborne CK, Wu M-F, Hilsenbeck SG, Pavlick A, Zhang X, Chamness GC, Wong H, Rosen J, Chang JC**. 2008. Intrinsic Resistance of Tumorigenic Breast Cancer Cells to Chemotherapy. J Natl Cancer Inst **100**:672–679.

4. **Singh A, Settleman J**. 2010. EMT, cancer stem cells and drug resistance: an emerging axis of evil in the war on cancer. Oncogene **29**:4741–4751.

5. **Valent P, Bonnet D, De Maria R, Lapidot T, Copland M, Melo JV, Chomienne C, Ishikawa F, Schuringa JJ, Stassi G, Huntly B, Herrmann H, Soulier J, Roesch A, Schuurhuis GJ, Wöhrer S, Arock M, Zuber J, Cerny-Reiterer S, Johnsen HE, Andreeff M, Eaves C**. 2012. Cancer stem cell definitions and terminology: the devil is in the details. Nat Rev Cancer **12**:767–775.

6. **Reya T, Morrison SJ, Clarke MF, Weissman IL**. 2001. Stem cells, cancer, and cancer stem cells. Nature **414**:105–111.

7. **Wicha MS, Liu S, Dontu G**. 2006. Cancer stem cells: an old idea--a paradigm shift. Cancer Res **66**:1883–1890; discussion 1895–1896.

8. **Lapidot T, Sirard C, Vormoor J, Murdoch B, Hoang T, Caceres-Cortes J, Minden M, Paterson B, Caligiuri MA, Dick JE**. 1994. A cell initiating human acute myeloid leukaemia after transplantation into SCID mice. Nature **367**:645–648.

9. **Al-Hajj M, Wicha MS, Benito-Hernandez A, Morrison SJ, Clarke MF**. 2003. Prospective identification of tumorigenic breast cancer cells. Proc Natl Acad Sci **100**:3983–3988.

10. **O'Brien CA, Pollett A, Gallinger S, Dick JE**. 2007. A human colon cancer cell capable of initiating tumour growth in immunodeficient mice. Nature **445**:106–110.

11. **Zhang M, Behbod F, Atkinson RL, Landis MD, Kittrell F, Edwards D, Medina D, Tsimelzon A, Hilsenbeck S, Green JE, Michalowska AM, Rosen JM**. 2008. Identification of tumor-initiating cells in a p53-null mouse model of breast cancer. Cancer Res **68**:4674–4682.

12. **Bonnet D, Dick JE**. 1997. Human acute myeloid leukemia is organized as a hierarchy that originates from a primitive hematopoietic cell. Nat Med **3**:730–737.

13. **Liu G, Yuan X, Zeng Z, Tunici P, Ng H, Abdulkadir IR, Lu L, Irvin D, Black KL, Yu JS**. 2006. Analysis of gene expression and chemoresistance of CD133+ cancer stem cells in glioblastoma. Mol Cancer **5**:67.

14. **Dylla SJ, Beviglia L, Park I-K, Chartier C, Raval J, Ngan L, Pickell K, Aguilar J, Lazetic S, Smith-Berdan S, Clarke MF, Hoey T, Lewicki J, Gurney AL**. 2008. Colorectal cancer stem cells are enriched in xenogeneic tumors following chemotherapy. PloS One **3**:e2428.

15. **Alvero AB, Chen R, Fu H-H, Montagna M, Schwartz PE, Rutherford T, Silasi D-A, Steffensen KD, Waldstrom M, Visintin I, Mor G**. 2009. Molecular phenotyping of human ovarian cancer stem cells unravels the mechanisms for repair and chemoresistance. Cell Cycle Georget Tex **8**:158–166.

16. **Todaro M, Alea MP, Di Stefano AB, Cammareri P, Vermeulen L, Iovino F, Tripodo C, Russo A, Gulotta G, Medema JP, Stassi G**. 2007. Colon cancer stem cells dictate tumor growth and resist cell death by production of interleukin-4. Cell Stem Cell **1**:389–402.

17. **Ma S, Lee TK, Zheng B-J, Chan KW, Guan X-Y**. 2008. CD133+ HCC cancer stem cells confer chemoresistance by preferential expression of the Akt/PKB survival pathway. Oncogene **27**:1749–1758.

18. **Litman T, Brangi M, Hudson E, Fetsch P, Abati A, Ross DD, Miyake K, Resau JH, Bates SE**. 2000. The multidrug-resistant phenotype associated with overexpression of the new ABC half-transporter, MXR (ABCG2). J Cell Sci **113 (Pt 11)**:2011–2021.

19. **Bao S, Wu Q, McLendon RE, Hao Y, Shi Q, Hjelmeland AB, Dewhirst MW, Bigner DD, Rich JN**. 2006. Glioma stem cells promote radioresistance by preferential activation of the DNA damage response. Nature **444**:756–760.

20. **Zhang B, Strauss AC, Chu S, Li M, Ho Y, Shiang K-D, Snyder DS, Huettner CS, Shultz L, Holyoake T, Bhatia R**. 2010. Effective targeting of quiescent chronic myelogenous leukemia stem cells by histone deacetylase inhibitors in combination with imatinib mesylate. Cancer Cell **17**:427–442.

21. **Sharma SV, Lee DY, Li B, Quinlan MP, Takahashi F, Maheswaran S, McDermott U, Azizian N, Zou L, Fischbach MA, Wong K-K, Brandstetter K, Wittner B, Ramaswamy S, Classon M, Settleman J**. 2010. A chromatin-mediated reversible drug-tolerant state in cancer cell subpopulations. Cell **141**:69–80.

22. **Ginestier C, Hur MH, Charafe-Jauffret E, Monville F, Dutcher J, Brown M, Jacquemier J, Viens P, Kleer CG, Liu S, Schott A, Hayes D, Birnbaum D, Wicha MS, Dontu G**. 2007. ALDH1 is a marker of normal and malignant human mammary stem cells and a predictor of poor clinical outcome. Cell Stem Cell **1**:555–567.

23. **Ricardo S, Vieira AF, Gerhard R, Leitão D, Pinto R, Cameselle-Teijeiro JF, Milanezi F, Schmitt F, Paredes J**. 2011. Breast cancer stem cell markers CD44, CD24 and ALDH1: expression distribution within intrinsic molecular subtype. J Clin Pathol **64**:937–946.

24. **Jaggupilli A, Elkord E**. 2012. Significance of CD44 and CD24 as Cancer Stem Cell Markers: An Enduring Ambiguity. J Immunol Res **2012**:e708036.

25. **Yang J, Weinberg RA**. 2008. Epithelial-Mesenchymal Transition: At the Crossroads of Development and Tumor Metastasis. Dev Cell **14**:818–829.

26. **Greenburg G, Hay ED**. 1982. Epithelia suspended in collagen gels can lose polarity and express characteristics of migrating mesenchymal cells. J Cell Biol **95**:333–339.

27. **Mani SA, Guo W, Liao M-J, Eaton EN, Ayyanan A, Zhou AY, Brooks M, Reinhard F, Zhang CC, Shipitsin M, Campbell LL, Polyak K, Brisken C, Yang J, Weinberg RA**. 2008. The epithelial-mesenchymal transition generates cells with properties of stem cells. Cell **133**:704–715.

28. **Polyak K, Weinberg RA**. 2009. Transitions between epithelial and mesenchymal states: acquisition of malignant and stem cell traits. Nat Rev Cancer **9**:265–273.

29. **Santisteban M, Reiman JM, Asiedu MK, Behrens MD, Nassar A, Kalli KR, Haluska P, Ingle JN, Hartmann LC, Manjili MH, Radisky DC, Ferrone S, Knutson KL**. 2009. Immune-induced epithelial to mesenchymal transition in vivo generates breast cancer stem cells. Cancer Res **69**:2887–2895.

30. **Ben-Porath I, Thomson MW, Carey VJ, Ge R, Bell GW, Regev A, Weinberg RA**. 2008. An embryonic stem cell-like gene expression signature in poorly differentiated aggressive human tumors. Nat Genet **40**:499–507.

31. **Tsai JH, Donaher JL, Murphy DA, Chau S, Yang J**. 2012. Spatiotemporal Regulation of Epithelial-Mesenchymal Transition Is Essential for Squamous Cell Carcinoma Metastasis. Cancer Cell **22**:725–736.

32. **Ocaña OH, Córcoles R, Fabra Á, Moreno-Bueno G, Acloque H, Vega S, Barrallo-Gimeno A, Cano A, Nieto MA**. 2012. Metastatic Colonization Requires the Repression of the Epithelial-Mesenchymal Transition Inducer Prrx1. Cancer Cell **22**:709–724.

33. **Chao YL, Shepard CR, Wells A**. 2010. Breast carcinoma cells re-express E-cadherin during mesenchymal to epithelial reverting transition. Mol Cancer **9**:179.

34. **Brabletz T, Jung A, Reu S, Porzner M, Hlubek F, Kunz-Schughart LA, Knuechel R, Kirchner T**. 2001. Variable beta-catenin expression in colorectal cancers indicates tumor progression driven by the tumor environment. Proc Natl Acad Sci U S A **98**:10356–10361.

35. **Hudson LG, Zeineldin R, Stack MS**. 2008. Phenotypic plasticity of neoplastic ovarian epithelium: unique cadherin profiles in tumor progression. Clin Exp Metastasis **25**:643–655.

36. **Chaffer CL, Brennan JP, Slavin JL, Blick T, Thompson EW, Williams ED**. 2006. Mesenchymal-to-epithelial transition facilitates bladder cancer metastasis: role of fibroblast growth factor receptor-2. Cancer Res **66**:11271–11278.

37. **LaGamba D, Nawshad A, Hay ED**. 2005. Microarray analysis of gene expression during epithelial-mesenchymal transformation. Dev Dyn Off Publ Am Assoc Anat **234**:132–142.

38. **Hong K-O, Kim J-H, Hong J-S, Yoon H-J, Lee J-I, Hong S-P, Hong S-D**. 2009. Inhibition of Akt activity induces the mesenchymal-to-epithelial reverting transition with restoring E-cadherin expression in KB and KOSCC-25B oral squamous cell carcinoma cells. J Exp Clin Cancer Res **28**:28.

39. **Mege RM, Matsuzaki F, Gallin WJ, Goldberg JI, Cunningham BA, Edelman GM**. 1988. Construction of epithelioid sheets by transfection of mouse sarcoma cells with cDNAs for chicken cell adhesion molecules. Proc Natl Acad Sci **85**:7274–7278.

40. **Bae G-Y, Choi S-J, Lee J-S, Jo J, Lee J, Kim J, Cha H-J**. 2013. Loss of E-cadherin activates EGFR-MEK/ERK signaling, which promotes invasion via the ZEB1/MMP2 axis in non-small cell lung cancer. Oncotarget **4**:2512–2522.

41. **Zheng G, Lyons JG, Tan TK, Wang Y, Hsu T-T, Min D, Succar L, Rangan GK, Hu M, Henderson BR, Alexander SI, Harris DCH**. 2009. Disruption of E-Cadherin by Matrix Metalloproteinase Directly Mediates Epithelial-Mesenchymal Transition Downstream of Transforming Growth Factor-β1 in Renal Tubular Epithelial Cells. Am J Pathol **175**:580–591.

42. **Laux H, Tomer R, Mader MT, Smida J, Budczies J, Kappler R, Hahn H, Blöchinger M, Schnitzbauer U, Eckardt-Schupp F, Höfler H, Becker K-F**. 2004. Tumor-associated E-cadherin mutations do not induce Wnt target gene expression, but affect E-cadherin repressors. Lab Investig J Tech Methods Pathol **84**:1372–1386.

43. **Hennig G, Behrens J, Truss M, Frisch S, Reichmann E, Birchmeier W**. 1995. Progression of carcinoma cells is associated with alterations in chromatin structure and factor binding at the E-cadherin promoter in vivo. Oncogene **11**:475–484.

44. **Hajra KM, Ji X, Fearon ER**. 1999. Extinction of E-cadherin expression in breast cancer via a dominant repression pathway acting on proximal promoter elements. Oncogene **18**:7274–7279.

45. **Tamura G, Yin J, Wang S, Fleisher AS, Zou T, Abraham JM, Kong D, Smolinski KN, Wilson KT, James SP, Silverberg SG, Nishizuka S, Terashima M, Motoyama T, Meltzer SJ**. 2000. E-Cadherin gene promoter hypermethylation in primary human gastric carcinomas. J Natl Cancer Inst **92**:569–573.

46. **Witta SE, Gemmill RM, Hirsch FR, Coldren CD, Hedman K, Ravdel L, Helfrich B, Dziadziuszko R, Chan DC, Sugita M, Chan Z, Baron A, Franklin W, Drabkin HA, Girard L, Gazdar AF, Minna JD, Bunn PA**. 2006. Restoring E-Cadherin Expression Increases Sensitivity to Epidermal Growth Factor Receptor Inhibitors in Lung Cancer Cell Lines. Cancer Res **66**:944–950.

47. **Tryndyak VP, Beland FA, Pogribny IP**. 2010. E-cadherin transcriptional down-regulation by epigenetic and microRNA-200 family alterations is related to mesenchymal and drug-resistant phenotypes in human breast cancer cells. Int J Cancer **126**:2575–2583.

48. **Nam J-S, Ino Y, Sakamoto M, Hirohashi S**. 2002. Src Family Kinase Inhibitor PP2 Restores the E-Cadherin/Catenin Cell Adhesion System in Human Cancer Cells and Reduces Cancer Metastasis. Clin Cancer Res **8**:2430–2436.

49. **Deisboeck TS, Couzin ID**. 2009. Collective behavior in cancer cell populations. BioEssays **31**:190–197.

50. **Manuel Iglesias J, Beloqui I, Garcia-Garcia F, Leis O, Vazquez-Martin A, Eguiara A, Cufi S, Pavon A, Menendez JA, Dopazo J, Martin AG**. 2013. Mammosphere formation in breast carcinoma cell lines depends upon expression of E-cadherin. PloS One **8**:e77281.

51. **Sundfeldt K, Piontkewitz Y, Ivarsson K, Nilsson O, Hellberg P, Brännström M, Janson PO, Enerback S, Hedin L**. 1997. E-cadherin expression in human epithelial ovarian cancer and normal ovary. Int J Cancer J Int Cancer **74**:275–280.

52. **Rakha EA, Teoh TK, Lee AHS, Nolan CC, Ellis IO, Green AR**. 2013. Further evidence that E-cadherin is not a tumour suppressor gene in invasive ductal carcinoma of the breast: an immunohistochemical study. Histopathology **62**:695–701.

53. **Hough CD, Sherman-Baust CA, Pizer ES, Montz FJ, Im DD, Rosenshein NB, Cho KR, Riggins GJ, Morin PJ**. 2000. Large-Scale Serial Analysis of Gene Expression Reveals Genes Differentially Expressed in Ovarian Cancer. Cancer Res **60**:6281–6287.

54. **Li L, Wang S, Jezierski A, Moalim-Nour L, Mohib K, Parks RJ, Retta SF, Wang L**. 2010. A unique interplay between Rap1 and E-cadherin in the endocytic pathway regulates self-renewal of human embryonic stem cells. Stem Cells Dayt Ohio **28**:247–257.

55. **Li L, Wang BH, Wang S, Moalim-Nour L, Mohib K, Lohnes D, Wang L**. 2010. Individual cell movement, asymmetric colony expansion, rho-associated kinase, and E-cadherin impact the clonogenicity of human embryonic stem cells. Biophys J **98**:2442–2451.

56. **Peluso JJ, Pappalardo A, Fernandez G**. 2001. E-Cadherin-Mediated Cell Contact Prevents Apoptosis of Spontaneously Immortalized Granulosa Cells by Regulating Akt Kinase Activity. Biol Reprod **64**:1183–1190.

57. **Reddy P, Liu L, Ren C, Lindgren P, Boman K, Shen Y, Lundin E, Ottander U, Rytinki M, Liu K**. 2005. Formation of E-Cadherin-Mediated Cell-Cell Adhesion Activates Akt and Mitogen Activated Protein Kinase via Phosphatidylinositol 3 Kinase and Ligand-Independent Activation of Epidermal Growth Factor Receptor in Ovarian Cancer Cells. Mol Endocrinol **19**:2564–2578.

58. **Pece S, Chiariello M, Murga C, Gutkind JS**. 1999. Activation of the protein kinase Akt/PKB by the formation of E-cadherin-mediated cell-cell junctions. Evidence for the association of phosphatidylinositol 3-kinase with the E-cadherin adhesion complex. J Biol Chem **274**:19347–19351.

59. **Thompson EW, Haviv I**. 2011. The social aspects of EMT-MET plasticity. Nat Med **17**:1048–1049.

60. **Nusse R, Varmus HE**. 1992. Wnt genes. Cell **69**:1073–1087.

61. **Komiya Y, Habas R**. 2008. Wnt signal transduction pathways. Organogenesis **4**:68–75.

62. **Gordon MD, Nusse R**. 2006. Wnt Signaling: Multiple Pathways, Multiple Receptors, and Multiple Transcription Factors. J Biol Chem **281**:22429–22433.

63. **MacDonald BT, Tamai K, He X**. 2009. Wnt/β-catenin signaling: components, mechanisms, and diseases. Dev Cell **17**:9–26.

64. **Nelson WJ, Nusse R**. 2004. Convergence of Wnt, β-Catenin, and Cadherin Pathways. Science **303**:1483–1487.

65. **Huang T-S, Li L, Moalim-Nour L, Jia D, Bai J, Yao Z, Bennett SAL, Figeys D, Wang L**. 2015. A Regulatory Network Involving β-Catenin, e-Cadherin, PI3k/Akt, and Slug Balances Self-Renewal and Differentiation of Human Pluripotent Stem Cells In Response to Wnt Signaling. STEM CELLS **33**:1419–1433.

66. **Bienz M**. 2005. β-Catenin: A Pivot between Cell Adhesion and Wnt Signalling. Curr Biol **15**:R64–R67.

67. **Yook JI, Li X-Y, Ota I, Fearon ER, Weiss SJ**. 2005. Wnt-dependent Regulation of the E-cadherin Repressor Snail. J Biol Chem **280**:11740–11748.

68. **Orsulic S, Huber O, Aberle H, Arnold S, Kemler R**. 1999. E-cadherin binding prevents beta-catenin nuclear localization and beta-catenin/LEF-1-mediated transactivation. J Cell Sci **112 (Pt 8)**:1237–1245.

69. **Heuberger J, Birchmeier W**. 2010. Interplay of Cadherin-Mediated Cell Adhesion and Canonical Wnt Signaling. Cold Spring Harb Perspect Biol **2**:a002915.

70. **Wielenga VJ, Smits R, Korinek V, Smit L, Kielman M, Fodde R, Clevers H, Pals ST**. 1999. Expression of CD44 in Apc and Tcf mutant mice implies regulation by the WNT pathway. Am J Pathol **154**:515–523.

71. **Green JL, La J, Yum KW, Desai P, Rodewald L-W, Zhang X, Leblanc M, Nusse R, Lewis MT, Wahl GM**. 2013. Paracrine Wnt signaling both promotes and inhibits human breast tumor growth. Proc Natl Acad Sci **110**:6991–6996.

72. **Sato N, Meijer L, Skaltsounis L, Greengard P, Brivanlou AH**. 2004. Maintenance of pluripotency in human and mouse embryonic stem cells through activation of Wnt signaling by a pharmacological GSK-3-specific inhibitor. Nat Med **10**:55–63.

73. **Davidson KC, Adams AM, Goodson JM, McDonald CE, Potter JC, Berndt JD, Biechele TL, Taylor RJ, Moon RT**. 2012. Wnt/β-catenin signaling promotes differentiation, not self-renewal, of human embryonic stem cells and is repressed by Oct4. Proc Natl Acad Sci **109**:4485–4490.

74. **Aubert J, Dunstan H, Chambers I, Smith A**. 2002. Functional gene screening in embryonic stem cells implicates Wnt antagonism in neural differentiation. Nat Biotechnol **20**:1240–1245.

75. **Lluis F, Pedone E, Pepe S, Cosma MP**. 2008. Periodic Activation of Wnt/β-Catenin Signaling Enhances Somatic Cell Reprogramming Mediated by Cell Fusion. Cell Stem Cell **3**:493–507.

76. **Anastas JN, Moon RT**. 2013. WNT signalling pathways as therapeutic targets in cancer. Nat Rev Cancer **13**:11–26.

77. **Lejeune S, Huguet EL, Hamby A, Poulsom R, Harris AL**. 1995. Wnt5a cloning, expression, and up-regulation in human primary breast cancers. Clin Cancer Res Off J Am Assoc Cancer Res **1**:215–222.

78. **Saitoh T, Katoh M**. 2002. Expression and regulation of WNT5A and WNT5B in human cancer: up-regulation of WNT5A by TNFalpha in MKN45 cells and up-regulation of WNT5B by beta-estradiol in MCF-7 cells. Int J Mol Med **10**:345–349.

79. **Katoh M**. 2003. Expression and regulation of WNT1 in human cancer: up-regulation of WNT1 by beta-estradiol in MCF-7 cells. Int J Oncol **22**:209–212.

80. **Bilir B, Kucuk O, Moreno CS**. 2013. Wnt signaling blockage inhibits cell proliferation and migration, and induces apoptosis in triple-negative breast cancer cells. J Transl Med **11**:280.

81. **Pannequin J, Delaunay N, Buchert M, Surrel F, Bourgaux J, Ryan J, Boireau S, Coelho J, Pélegrin A, Singh P, Shulkes A, Yim M, Baldwin GS, Pignodel C, Lambeau G, Jay P, Joubert D, Hollande F**. 2007. β-Catenin/Tcf-4 Inhibition After Progastrin Targeting Reduces Growth and Drives Differentiation of Intestinal Tumors. Gastroenterology **133**:1554–1568.

82. **Liu J, Pan S, Hsieh MH, Ng N, Sun F, Wang T, Kasibhatla S, Schuller AG, Li AG, Cheng D, Li J, Tompkins C, Pferdekamper A, Steffy A, Cheng J, Kowal C, Phung V, Guo G, Wang Y, Graham MP, Flynn S, Brenner JC, Li C, Villarroel MC, Schultz PG, Wu X, McNamara P, Sellers WR, Petruzzelli L, Boral AL, Seidel HM, McLaughlin ME, Che J, Carey TE, Vanasse G, Harris JL**. 2013. Targeting Wnt-driven cancer through the inhibition of Porcupine by LGK974. Proc Natl Acad Sci U S A **110**:20224–20229.

83. **Ramachandran I, Ganapathy V, Gillies E, Fonseca I, Sureban SM, Houchen CW, Reis A, Queimado L**. 2014. Wnt inhibitory factor 1 suppresses cancer stemness and induces cellular senescence. Cell Death Dis **5**:e1246.

84. **Howard JC, Varallo VM, Ross DC, Roth JH, Faber KJ, Alman B, Gan BS**. 2003. Elevated levels of β-catenin and fibronectin in three-dimensional collagen cultures of Dupuytren's disease cells are regulated by tension in vitro. BMC Musculoskelet Disord **4**:16.

85. **Bellacosa A, Kumar CC, Di Cristofano A, Testa JR**. 2005. Activation of AKT kinases in cancer: implications for therapeutic targeting. Adv Cancer Res **94**:29–86.

86. **Martelli AM, Tabellini G, Bressanin D, Ognibene A, Goto K, Cocco L, Evangelisti C**. 2012. The emerging multiple roles of nuclear Akt. Biochim Biophys Acta BBA - Mol Cell Res **1823**:2168–2178.

87. **Engelman JA**. 2009. Targeting PI3K signalling in cancer: opportunities, challenges and limitations. Nat Rev Cancer **9**:550–562.

88. **Vivanco I, Sawyers CL**. 2002. The phosphatidylinositol 3-Kinase–AKT pathway in human cancer. Nat Rev Cancer **2**:489–501.

89. **Zhao N, Wilkerson MD, Shah U, Yin X, Wang A, Hayward MC, Roberts P, Lee CB, Parsons AM, Thorne LB, Haithcock BE, Grilley-Olson JE, Stinchcombe TE, Funkhouser WK, Wong K-K, Sharpless NE, Hayes DN**. 2014. Alterations of LKB1 and KRAS and risk of brain metastasis: comprehensive characterization by mutation analysis, copy number, and gene expression in non-small-cell lung carcinoma. Lung Cancer Amst Neth **86**:255–261.

90. **Ruggeri BA, Huang L, Wood M, Cheng JQ, Testa JR**. 1998. Amplification and overexpression of the AKT2 oncogene in a subset of human pancreatic ductal adenocarcinomas. Mol Carcinog **21**:81–86.

91. **Pradella LM, Evangelisti C, Ligorio C, Ceccarelli C, Neri I, Zuntini R, Amato LB, Ferrari S, Martelli AM, Gasparre G, Turchetti D**. 2014. A novel deleterious PTEN mutation in a patient with early-onset bilateral breast cancer. BMC Cancer **14**:70.

92. **Seki N, Takasu T, Mandai K, Nakata M, Saeki H, Heike Y, Takata I, Segawa Y, Hanafusa T, Eguchi K**. 2002. Expression of eukaryotic initiation factor 4E in atypical adenomatous hyperplasia and adenocarcinoma of the human peripheral lung. Clin Cancer Res Off J Am Assoc Cancer Res **8**:3046–3053.

93. **Wang S, Rosenwald IB, Hutzler MJ, Pihan GA, Savas L, Chen JJ, Woda BA**. 1999. Expression of the eukaryotic translation initiation factors 4E and 2alpha in non-Hodgkin's lymphomas. Am J Pathol **155**:247–255.

94. **Samuels Y, Wang Z, Bardelli A, Silliman N, Ptak J, Szabo S, Yan H, Gazdar A, Powell SM, Riggins GJ, Willson JKV, Markowitz S, Kinzler KW, Vogelstein B, Velculescu VE**. 2004. High frequency of mutations of the PIK3CA gene in human cancers. Science **304**:554.

95. **Miwa W, Yasuda J, Murakami Y, Yashima K, Sugano K, Sekine T, Kono A, Egawa S, Yamaguchi K, Hayashizaki Y, Sekiya T**. 1996. Isolation of DNA sequences amplified at chromosome 19q13.1-q13.2 including the AKT2 locus in human pancreatic cancer. Biochem Biophys Res Commun **225**:968–974.

96. **Tsai L-H, Chen P-M, Cheng Y-W, Chen C-Y, Sheu G-T, Wu T-C, Lee H**. 2014. LKB1 loss by alteration of the NKX2-1/p53 pathway promotes tumor malignancy and predicts poor survival and relapse in lung adenocarcinomas. Oncogene **33**:3851–3860.

97. **Agarwal E, Chaudhuri A, Leiphrakpam PD, Haferbier KL, Brattain MG, Chowdhury S**. 2014. Akt inhibitor MK-2206 promotes anti-tumor activity and cell death by modulation of AIF and Ezrin in colorectal cancer. BMC Cancer **14**:145.

98. **Yang L, Dan HC, Sun M, Liu Q, Sun X, Feldman RI, Hamilton AD, Polokoff M, Nicosia SV, Herlyn M, Sebti SM, Cheng JQ**. 2004. Akt/protein kinase B signaling inhibitor-2, a selective small molecule inhibitor of Akt signaling with antitumor activity in cancer cells overexpressing Akt. Cancer Res **64**:4394–4399.

99. **Cheng JQ, Ruggeri B, Klein WM, Sonoda G, Altomare DA, Watson DK, Testa JR**. 1996. Amplification of AKT2 in human pancreatic cells and inhibition of AKT2 expression and tumorigenicity by antisense RNA. Proc Natl Acad Sci U S A **93**:3636–3641.

100. **Martelli AM, Tazzari PL, Tabellini G, Bortul R, Billi AM, Manzoli L, Ruggeri A, Conte R, Cocco L**. 2003. A new selective AKT pharmacological inhibitor reduces resistance to chemotherapeutic drugs, TRAIL, all-trans-retinoic acid, and ionizing radiation of human leukemia cells. Leukemia **17**:1794–1805.

101. **Rhodes N, Heerding DA, Duckett DR, Eberwein DJ, Knick VB, Lansing TJ, McConnell RT, Gilmer TM, Zhang S-Y, Robell K, Kahana JA, Geske RS, Kleymenova EV, Choudhry AE, Lai Z, Leber JD, Minthorn EA, Strum SL, Wood ER, Huang PS, Copeland RA, Kumar R**. 2008. Characterization of an Akt kinase inhibitor with potent pharmacodynamic and antitumor activity. Cancer Res **68**:2366–2374.

102. **Chun K-H, Kosmeder JW, Sun S, Pezzuto JM, Lotan R, Hong WK, Lee H-Y**. 2003. Effects of deguelin on the phosphatidylinositol 3-kinase/Akt pathway and apoptosis in premalignant human bronchial epithelial cells. J Natl Cancer Inst **95**:291–302.

103. **Heerding DA, Rhodes N, Leber JD, Clark TJ, Keenan RM, Lafrance LV, Li M, Safonov IG, Takata DT, Venslavsky JW, Yamashita DS, Choudhry AE, Copeland RA, Lai Z, Schaber MD, Tummino PJ, Strum SL, Wood ER, Duckett DR, Eberwein D, Knick VB, Lansing TJ, McConnell RT, Zhang S, Minthorn EA, Concha NO, Warren GL, Kumar R**. 2008. Identification of 4-(2-(4-amino-1,2,5-oxadiazol-3-yl)-1-ethyl-7-{[(3S)-3-piperidinylmethyl]oxy}-1H-imidazo[4,5-c]pyridin-4-yl)-2-methyl-3-butyn-2-ol (GSK690693), a novel inhibitor of AKT kinase. J Med Chem **51**:5663–5679.

104. **Livak KJ, Schmittgen TD**. 2001. Analysis of relative gene expression data using real-time quantitative PCR and the 2(-Delta Delta C(T)) Method. Methods San Diego Calif **25**:402–408.

105. **Takahashi K, Yamanaka S**. 2006. Induction of Pluripotent Stem Cells from Mouse Embryonic and Adult Fibroblast Cultures by Defined Factors. Cell **126**:663–676.

106. **Leis O, Eguiara A, Lopez-Arribillaga E, Alberdi MJ, Hernandez-Garcia S, Elorriaga K, Pandiella A, Rezola R, Martin AG**. 2012. Sox2 expression in breast tumours and activation in breast cancer stem cells. Oncogene **31**:1354–1365.

107. **Luo W, Li S, Peng B, Ye Y, Deng X, Yao K**. 2013. Embryonic Stem Cells Markers SOX2, OCT4 and Nanog Expression and Their Correlations with Epithelial-Mesenchymal Transition in Nasopharyngeal Carcinoma. PLoS ONE **8**:e56324.

108. **Borowicz S, Van Scoyk M, Avasarala S, Karuppusamy Rathinam MK, Tauler J, Bikkavilli RK, Winn RA**. 2014. The soft agar colony formation assay. J Vis Exp JoVE e51998.

109. **Cao L, Zhou Y, Zhai B, Liao J, Xu W, Zhang R, Li J, Zhang Y, Chen L, Qian H, Wu M, Yin Z**. 2011. Sphere-forming cell subpopulations with cancer stem cell properties in human hepatoma cell lines. BMC Gastroenterol **11**:71.

110. **Rosenblum ML, Knebel KD, Wheeler KT, Barker M, Wilson CB**. 1975. Development of an in vitro colony formation assay for the evaluation of in vivo chemotherapy of a rat brain tumor. In Vitro **11**:264–273.

111. **Alley MC, Uhl CB, Lieber MM**. 1982. Improved detection of drug cytotoxicity in the soft agar colony formation assay through use of a metabolizable tetrazolium salt. Life Sci **31**:3071–3078.

112. **Green SK, Francia G, Isidoro C, Kerbel RS**. 2004. Antiadhesive antibodies targeting E-cadherin sensitize multicellular tumor spheroids to chemotherapy in vitro. Mol Cancer Ther **3**:149–159.

113. **Navarro P, Gómez M, Pizarro A, Gamallo C, Quintanilla M, Cano A**. 1991. A role for the E-cadherin cell-cell adhesion molecule during tumor progression of mouse epidermal carcinogenesis. J Cell Biol **115**:517–533.

114. **Kang H-G, Jenabi JM, Zhang J, Keshelava N, Shimada H, May WA, Ng T, Reynolds CP, Triche TJ, Sorensen PHB**. 2007. E-Cadherin Cell-Cell Adhesion in Ewing Tumor Cells Mediates Suppression of Anoikis through Activation of the ErbB4 Tyrosine Kinase. Cancer Res **67**:3094–3105.

115. **Teo J-L, Kahn M**. 2010. The Wnt signaling pathway in cellular proliferation and differentiation: A tale of two coactivators. Adv Drug Deliv Rev **62**:1149–1155.

116. **El-Tanani MK, Barraclough R, Wilkinson MC, Rudland PS**. 2001. Regulatory region of metastasis-inducing DNA is the binding site for T cell factor-4. Publ Online 30 March 2001 Doi101038sjonc1204358 **20**.

117. **Ravindranath A, Yuen H-F, Chan K-K, Grills C, Fennell DA, Lappin TR, El-Tanani M**. 2011. Wnt–β-catenin–Tcf-4 signalling-modulated invasiveness is dependent on osteopontin expression in breast cancer. Br J Cancer **105**:542–551.

118. **Shulewitz M, Soloviev I, Wu T, Koeppen H, Polakis P, Sakanaka C**. 2006. Repressor roles for TCF-4 and Sfrp1 in Wnt signaling in breast cancer. Oncogene **25**:4361–4369.

119. **Mestdagt M, Polette M, Buttice G, Noël A, Ueda A, Foidart J-M, Gilles C**. 2006. Transactivation of MCP-1/CCL2 by β-catenin/TCF-4 in human breast cancer cells. Int J Cancer **118**:35–42.

120. **Kerr JFR, Wyllie AH, Currie AR**. 1972. Apoptosis: A Basic Biological Phenomenon with Wide-ranging Implications in Tissue Kinetics. Br J Cancer **26**:239–257.

121. **Elmore S**. 2007. Apoptosis: A Review of Programmed Cell Death. Toxicol Pathol **35**:495–516.

122. **Proskuryakov SY a, Konoplyannikov AG, Gabai VL**. 2003. Necrosis: a specific form of programmed cell death? Exp Cell Res **283**:1–16.

123. **Golstein P, Kroemer G**. 2007. Cell death by necrosis: towards a molecular definition. Trends Biochem Sci **32**:37–43.

6. APPENDICES

Map of the pLVX-Tet-On Advanced Vector.

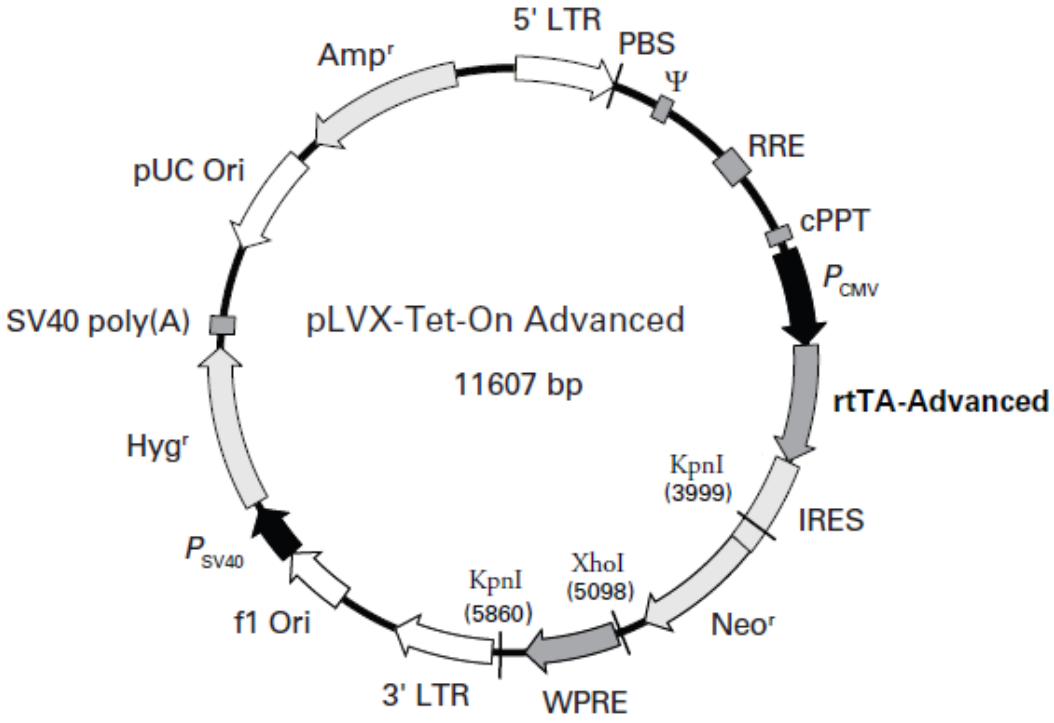

Map of the pLVX-Tight-Puro Vector.